adrenomedullin gene. *Circulation* 2001; **104**: 1964–1971.
27. Ishimitsu T, Tsukada K, Minami J, *et al*: Microsatellite DNA polymorphism of human adrenomedullin gene in type 2 diabetic patients with renal failure. *Kidney Int* 2003; **63**: 2230–2235.
28. Nishikimi T, Mori Y, Kobayashi N, *et al*: Renoprotective effect of chronic adrenomedullin infusion in Dahl salt-sensitive rats. *Hypertension* 2002; **39**: 1077–1082.
29. Kubo A, Kurioka H, Minamino N, *et al*: Plasma and urinary levels of adrenomedullin in chronic glomerulonephritis patients with proteinuria. *Nephron* 1998; **80**: 227–230.

Genotype and Haplotype Association Study of the *STRK1* Region on 5q12 Among Japanese

A Case-Control Study

Tomohiro Nakayama, MD, PhD; Satoshi Asai, MD, PhD;
Naoyuki Sato, BAgr; Masayoshi Soma, MD, PhD

Background and Purpose—Cerebral infarction is thought to be a multifactorial disease that is affected by several environmental factors and genetic variants. Gretarsdottir et al identified a candidate locus (*STRK1*) for cerebral infarction with a significant logarithm of odds score at 5q12 in whites in 2002 and subsequently identified the *PDE4D* gene as a susceptibility gene at this locus in 2003. The aims of this haplotype-based case-control study were to confirm, using microsatellite markers and single-nucleotide polymorphisms (SNPs), whether *PDE4D* is also a susceptibility gene for cerebral infarction in Japanese subjects.

Methods—Cerebral infarction was defined as noncardiogenic ischemic stroke with signs and symptoms lasting >1 month in duration. We genotyped 208 Japanese cerebral infarction patients and 270 non–cerebral infarction controls for 31 SNPs, 3 dinucleotide microsatellites, and 1 tetranucleotide variable number of tandem repeat. Haplotypes were constructed and their frequencies compared between the cerebral infarction patients and the controls.

Results—The haplotype-based case-control study revealed that in addition to the region of the *PDE4D* gene ($P=0.002$), another region ($P<0.001$) also existed within the *STRK1* locus.

Conclusions—The region of the *PDE4D* gene and the other newly detected region within the *STRK1* locus were associated with cerebral infarction. (***Stroke*. 2006;37:69-76.**)

Key Words: case-control studies ■ cerebral infarction ■ genetics ■ haplotypes

Cerebral infarction is thought to be a heterogeneous multifactorial disease with which several environmental and genetic variants can be associated. These environmental and genetic factors together lead to the development of cerebral infarction.[1] Various susceptibility polymorphisms and mutations exert their effects in a polygenic manner. Epidemiologic studies have suggested a polygenic basis for cerebral infarction.[2] Identification of cerebral infarction susceptibility genes might enhance prediction of the risk of the disease. However, few genes considered as confirmed susceptibility genes for cerebral infarction have been identified.

Recently, Gretarsdottir et al[3] performed a genome-wide scan for susceptibility genes for stroke, which included ischemic and hemorrhagic stroke types, and identified a candidate locus with a significant logarithm of odds (LOD) score at the locus on 5q12 in whites. They named this locus *STRK1* because it did not correspond to any other previously known loci. Subsequently, they were able to identify the *PDE4D* gene as a susceptibility gene within this locus.[4] However, 2 questions need to be addressed. The first is whether *PDE4D* is a susceptibility gene for cerebral infarction in Japanese as well as whites, and the second is whether susceptibility genes other than *PD4ED* are present in the *STRK1* susceptibility region.

The aims of the present study were to determine whether *PDE4D* is a susceptibility gene for cerebral infarction in Japanese subjects using microsatellite markers and single-nucleotide polymorphisms (SNPs) in a haplotype-based case-control study and also to elucidate whether it is the only susceptibility gene in the *STRK1* locus on 5q12.

Methods

Subjects

Patients and control subjects from the northern area of Tokyo were recruited for the case-control study. Patients were selected among those who were admitted at our hospital (Nihon University Hospital in Tokyo) or community hospitals in Tokyo between 1995 and 2005. Control subjects were selected from among the outpatients at our hospital during the same period. More than 80% of the ≈500 subjects we approached consented to participate in the study. Therefore, given that the subjects were selected according to the criteria for case-control studies, this investigation cannot be considered a population-based study. The study group consisted of 208 patients (126 men and 82 women; mean age

Received July 26, 2005; final revision received September 20, 2005; accepted October 17, 2005.

From the Divisions of Receptor Biology (T.N., N.S.) and Genomic Epidemiology and Clinical Trials (S.A.), Advanced Medical Research Center, and Division of Nephrology and Endocrinology (M.S.), Department of Medicine, Nihon University School of Medicine, Tokyo, Japan.

Correspondence to Tomohiro Nakayama, MD, Division of Receptor Biology, Advanced Medical Research Center, Nihon University School of Medicine, Ooyaguchi-kamimachi, 30-1 Itabashi-ku, Tokyo 173-8610, Japan. E-mail tnakayam@med.nihon-u.ac.jp

Stroke is available at http://www.strokeaha.org

DOI: 10.1161/01.STR.0000194961.17292.33

66.0±12.4 years, ranging from 29 to 99 years) diagnosed with cerebral infarction by computed tomography or MRI. All patients had neurological deficits that persisted for ≥1 month. A total of 270 subjects without cerebral infarction (141 men and 129 women; mean age 66.1±5.8 years, ranging from 50 to 98 years) were used as control subjects. Ages of the control subjects exceeded 50 years, but there was no significant difference between the cerebral infarction patients and the controls. Control subjects had vascular risk factors such as hypertension, diabetes mellitus, or hypercholesterolemia but no cerebrovascular disease. Hypertension was defined as having a sitting systolic blood pressure >160 mm Hg, diastolic blood pressure >100 mm Hg, or both on 3 occasions within 2 months after the first medical examination[5] or current use of an antihypertensive drug because of a history of arterial hypertension. Diagnosis of diabetes mellitus was based on the World Health Organization (WHO) criteria. Hyperlipidemia was defined as plasma total cholesterol >6.5 mmol, plasma triglycerides >2 mmol, or current use of a lipid-lowering drug in addition to a confirmed diagnosis of hyperlipidemia.[6] Smokers were defined as current or former smokers, whereas nonsmokers were defined as subjects with no history of previous or current smoking. History of smoking was recorded and current smokers included individuals who had stopped smoking <1 year before enrollment. History of alcohol use was recorded with habitual consumers defined as individuals who had ≥2 alcoholic beverages per day.[7] Individuals with a proven cause of cardioembolism such as recent myocardial infarction, valvular heart disease, and arrhythmia including atrial fibrillation were excluded from the cerebral infarction and control groups. Informed consent was obtained from each participant according to a protocol approved by the human studies committee at Nihon University.[8]

Biochemical Analysis

Plasma concentrations of total and high-density lipoprotein cholesterol and serum concentrations of creatinine and uric acid were measured as described previously.[7]

Genotyping of Microsatellite Markers and SNPs

Blood samples were collected from all participants, and genomic DNA was extracted from peripheral blood mononuclear cells using standard procedures.[9]

The entire *STRK1* locus is located between the D5S407 and D5S647 microsatellite markers. We therefore selected 3 microsatellite markers including 2 within the *STRK1* locus that were obtained using PRISM linkage mapping set HD-5 (Applied Biosystems). The primer sets supplied with this kit are suitable for accurate genotyping. The distance between neighboring microsatellite markers was an average of 4.5 cM, and the average heterozygosity was 0.76. The primers were dye-conjugated with FAM, HEX, or NED (Applied Biosystems). Polymerase chain reaction (PCR) amplification was performed using 15 ng of genomic DNA, 3 μL True Allele PCR Premix (containing PCR buffer, $MgCl_2$, dNTP, and AmpliTaq Gold; Applied Biosystems), and 0.33 μL of primer mix, to give a total reaction volume of 5 μL. PCR amplification consisted of an initial step at 95°C for 12 minutes to activate the AmpliTaq Gold; 10 cycles of denaturation at 94°C for 15 s, annealing at 55°C for 15 s, and extension at 72°C for 30 s. This was followed by 20 cycles of denaturation at 89°C for 15 s, annealing at 55°C for 15 s, and extension at 72°C for 30 s, with a final step at 72°C for 10 minutes. PCR amplification was performed using Gene Amp PCR 9600 thermocycler (Applied Biosystems). Products from up to 8 different PCRs were diluted 1:10 (1:5 for products labeled with HEX and NED) and pooled. The pooled products (1 μL) were then mixed with GS-500 LIZ internal size standard (0.5 μL) and diluted 1:6 with HI-DI formamide (Applied Biosystems). The pooled reactions were denatured at 95°C for 3 minutes and were loaded on an ABI 3700 DNA analyzer (Applied Biosystems). Fluorescent signals of fragments from the reactions with various fluorescent dyes were recorded and analyzed using GeneScan software version 2.1 (Applied Biosystems), and the sizes of the fluorescent peaks were estimated by referencing the in-lane size standards. Marker allele calling was performed using Genotyper software version 2 (Applied Biosystems). In addition, we performed a manual surveillance for all of the genotypes.[10]

To determine the associations between the markers and cerebral infarction, we selected 29 SNPs in the *STRK1* locus (supplemental Figure I, available online at http://stroke.ahajournals.org). Based on the website from the National Center for Biotechnology Information SNP database or the Applied Biosystems–Celera Discovery System (CDS) database, we chose SNPs that had a minor allele frequency >18%. SNP Assays-on-Demand kits (Applied Biosystems) were used for the determinations. The CDS was used to confirm the SNPs via the accession number. Genotypes were determined using TaqMan PCR.[11]

To examine whether *PDE4D* was the susceptibility gene for cerebral infarction in Japanese subjects, 2 SNPs (SNP45 and SNP83) and 1 tetranucleotide variable number of tandem repeat (VNTR; AC008818-1) were also genotyped because they had been reported previously to be susceptibility variants in the *PDE4D* gene.[4] X allele has been defined in a previous report.[4]

Linkage Disequilibrium Analysis and the Haplotype-Based Case-Control Study

Based on the genotype data of the genetic variations, linkage disequilibrium (LD) analysis was performed using SNPAlyze software (limited version 4.1; Dynacom Co, Ltd)[13] Haplotype frequencies were estimated by SNPAlyze software (version 3.2; Dynacom) using the expectation maximization algorithm.[12] Although the software was suitable for haplotype-based case-control studies using a maximum of 10 SNPs, it was not so for studies using microsatellites. Given that the online haplotype database showed all haplotype blocks on 5q12 to have been constructed by SNPs located within 1000 kbp in Japanese subjects (Project Ensemble), the pair-wise LD analysis of this study was performed using SNP pairs separated by <1000 kbp. Absolute D′ values (|D′|) ≥0.3 were used to assign SNP locations to 1 haplotype block. Tagged SNPs were selected by omitting 1 SNP in SNP pairs showing $r^2 \geq 0.5$ for each haplotype block. Despite being limited to 3 variants, the haplotype-based case-control study that used mixed SNP and microsatellite data were performed using the SNPAlyze software (limited version 4.1).[13]

Statistical Analysis

Clinical data represented as mean±SD were first tested by ANOVA followed by Fisher's protected least significant difference test; P values <0.05 indicated a significant difference (Dr. SPSS II; SPSS Japan Inc).[14] Hardy–Weinberg equilibrium was assessed by χ^2 analysis (Dr. SPSS II).

The overall distribution of alleles between the cerebral infarction patients and controls was analyzed by χ^2 goodness-of-fit test using 2×2 contingency tables; P values <0.05 were considered significant (Dr. SPSS II).[15]

In the haplotype-based case-control study, the threshold value for haplotype frequency that was included in the analysis was set at 2%.[16–19] All haplotype frequencies below the threshold value were excluded from the analysis, and P values <0.05/n were considered significant after correcting for the number of comparisons made (Bonferroni correction).[13]

Results

The characteristics of the study participants are shown in Table 1. Cerebral infarction and age-matched control groups were used to assess polymorphism association between and within sex-specific groups in the total study cohort.

Genotyping was successful for >97% of the samples using the 3 microsatellites, 1 VNTR, and 31 SNPs from the 478 study subjects. Although Gretarsdottir et al reported that SNP45 was one of the variants consistent with the susceptibility haplotype associated with cerebral infarction, none of the Japanese subjects in our experiment were heterogeneous for SNP45. The expected frequencies for each genotype for all 3 microsatellites and the remaining 30 SNPs in the control group were in Hardy–Weinberg equilibrium (data not shown). There was no associa-

TABLE 1. Characteristics of Study Participants

	Total			Men			Women		
	Non-Cerebral Infarction	Cerebral Infarction	*P* Value	Non-Cerebral Infarction	Cerebral Infarction	*P* Value	Non-Cerebral Infarction	Cerebral Infarction	*P* Value
No. of subjects	270	208		141	126		129	82	
Age (y)	66.1±5.8	66.0±12.4	0.958	64.2±8.1	64.4±11.6	0.818	68.1±11.6	68.5±13.3	0.851
BMI (kg/m^2)	23.6±3.9	22.7±5.4	0.080	22.7±3.5	22.6±4.7	0.067	23.5±4.3	22.8±6.8	0.524
SBP (mm Hg)	156.9±21.2	152.5±27.3	0.051	155.0±21.8	151.0±27.4	0.188	159.1±20.4	154.9±27.1	0.210
DBP (mm Hg)	90.9±14.5	86.8±16.0	0.004	90.4±14.1	87.9±16.5	0.176	91.4±15.0	85.0±15.2	0.004
Pulse (bpm)	73.9±11.6	77.0±14.3	0.012	73.1±11.5	76.8±14.6	0.029	74.8±11.8	77.4±13.8	0.161
Creatinine (mg/dL)	0.87±0.35	1.15±1.19	<0.001	1.01±0.39	1.25±1.13	0.026	0.73±0.22	1.02±1.27	0.015
Total cholesterol (mg/dL)	205.5±37.9	196.7±45.3	0.027	198.1±38.2	191.6±45.3	0.218	213.7±35.9	204.6±44.5	0.121
HDL cholesterol (mg/dL)	55.8±16.8	49.9±19.8	0.001	52.1±14.5	47.7±18.6	0.046	60.1±18.2	53.5±21.3	0.035
Uric acid (mg/dL)	5.40±1.48	5.67±2.28	0.131	5.96±1.42	6.06±2.01	0.668	4.77±1.27	5.06±2.54	0.301
Hypertension (%)	66.3	58.7	0.086	65.2	59.5	0.335	67.4	57.3	0.137
Diabetes mellitus (%)	13.3	19.7	0.060	14.2	18.3	0.367	12.4	22	0.066
Hypercholesterolemia (%)	43.2	44.1	0.852	26.2	31.8	0.322	48.1	46.3	0.807
Alcohol consumption (%)	15.7	16.0	0.940	25.7	25.7	0.999	3.3	2.0	0.644
Smoking (%)	32.7	45.1	0.021	47.4	63.0	0.031	14.0	17.6	0.558

BMI indicates body mass index; SBP, systolic blood pressure; DBP, diastolic blood pressure; HDL, high-density lipoprotein.

tion with any of the polymorphisms examined (after correcting for multiple comparisons; Table 2). The distribution of genotype data are shown in supplemental Table I.

LD patterns are illustrated by their |D'| and r^2 values (supplemental Table II). Seven haplotype blocks were found in the *STRK1* locus (Table 2). Tagged SNPs were selected in each haplotype block based on the pair-wise LD analysis. The haplotype-based case-control study that was performed for each block using tagged SNPs revealed that there were 2 significantly different haplotype blocks between the cerebral infarction and control groups (Table 2). Because 7 haplotype blocks were compared, *P* values <0.05/7=0.0071 were considered significant. The first block consisted of SNP83, SNP8, and VNTR within the *PDE4D* gene (*P*=0.002). The second block consisted of SNPs 18, 19, 20, and 21 (*P*<0.001). These *P* values also became significant after performing Bonferroni corrections.

SNP45, SNP83, VNTR, and the haplotype map built with SNP45 as well as the VNTR have all been reported previously to be associated with cerebral infarction.[4] SNP45 was not heterogenous, and the allelic distribution of SNP83 differed from that observed in whites.[4] The C allele was prevalent in 52.0% of the white control subjects but only in 11.8% of the Japanese control subjects. We performed our haplotype-based case-control study using SNP83, SNP8, and the VNTR because SNP45 was not polymorphic in our study population. The overall distribution of the haplotypes showed a significant difference between the cerebral infarction and control groups (χ^2=21.4; *P* value=0.002). The results for individual haplotypes showed that the frequency of the c-g-X haplotype was significantly higher in the cerebral infarction group compared with the controls (Table 3), whereas the T-g-X haplotype was significantly less frequent in the cerebral infarction group than in the controls.

Distribution of individual haplotypes in the second block and their *P* values are shown in Table 4. Results of the individual haplotypes indicated that 4 haplotypes exhibited significant differences between the cerebral infarction and control groups.

Discussion

The foundation for human studies examining putative causative genes that may be involved in cerebral infarction is based on a candidate gene approach. This involves selecting a functionally relevant gene to study and subsequently investigating its association with the cerebral infarction phenotype. Candidate genes in cerebral infarction research are chosen mainly for their role in the risk of stroke or vascular reactivity and brain response after insult. Stroke candidate genes fall into 5 main groups: renin-angiotensin system,[20] NO production,[21] lipid metabolism,[22] hemostasis,[23] and homocysteine metabolism.[24] However, the candidate regions are quite varied and the requisite assay analyses differ for each investigation.

A genome-wide scan was performed by Gretarsdottir et al in 2002 in an Icelandic population of 476 stroke patients and 438 relatives. The authors were able to identify a stroke susceptibility locus, *STRK1*, and mapped it to human chromosome 5q12.[3] A broad but rigorous definition of the phenotype was documented, and hemorrhagic stroke, ischemic stroke, and transient ischemic attack were all included to map a locus for common stroke. The LOD score at the chromosome 5 locus increased from an initial score of 2.00 to 3.39 after genotyping of 45 additional markers over the identified 45-cM region. Furthermore, linkage analysis undertaken using an even higher marker density resulted in an LOD score of 4.40. This study was therefore the first to successfully map a major locus for stroke by combining genealogy, a large population from which patients with broadly defined stroke were selected, and allele-sharing methods. Together, these considerations make this study one of the most comprehensive analyses of genetic predisposition to stroke published to

TABLE 2. Association Study of Microsatellites and SNPs

Variants					
Public ID	Celera ID		Gene Symbols	Position in Build 35.1	Distances Between Markers
D58407			MAP3K1	56 030 528	
					1 755 579
rs15009	C_2839927_1_	SNP1	FLK2	57 786 107	
					4 458
rs697133	C_8962862_1_	SNP2	PLK2	57 790 565	
					272 201
rs293009	C_1069038_10	SNP3	LOC115827	58 062 766	
					126 370
rs169854	C_3172290_10	SNP4	LOC115827	58 189 136	
					114 344
rs702531	C_2435134_10	SNP5	PDE4D	58 303 480	
					1 130
rs10075508	C_2435128_10	SNP6	PDE4D	58 304 610	
					49 012
rs1078368	C_2435061_10	SNP7	PDE4D	58 353 622	
					1 184 655
rs966221		SNP83	PDE4D	59 538 277	
					280 797
		SNP45	PDE4D	59 819 074	
					3 974
rs153031	C_3172890_1_	SNP8	PART1	59 823 048	
					2 066
AC008818-1		VNTR	PART1	59 825 114	
					380 980
rs3117	C_1153140_10	SNP9	FLJ12595	60 206 094	
					11 163
rs12522154	C_1150987_10	SNP10	FLJ12595	60 217 257	
					7 526
rs929780	C_8887869_1_	SNP11	FLJ12595	60 224 783	
					37 560
rs162228	C_1153167_10	SNP12	FLJ12595	60 262 343	
					286 980
rs34634	C_1144877_10	SNP13	LOC57399	60 549 323	
					1 092 001
rs2344396	C_1561870_10	SNP14	PRO2214	61 641 324	
					6 540
rs12515967	C_1394523_10	SNP15	PRO2214	61 647 864	
					82 272
rs247264	C_2386563_1_	SNP16	HSA9761	61 730 136	
					208 329
	C_1394796_10	SNP17	IPO11	61 938 465	
					1 000 405
D5S427			LOC441076	62 938 870	
					352 877
rs878567	C_8295923_10	SNP18	HTRIA	63 291 747	
					808 420

(Continued)

TABLE 2. (Continued)

Minor Allele Frequency		Odds Ratio	Allele		Haplotype			
Non-Cerebral Infarction	Cerebral Infarction	At-Risk Allele Cerebral Infarction	χ^2	*P* Value	Block	Tagged SNPs	χ^2	*P* Value
			22.690	0.020				
0.342	0.311	1.151	1.000	0.317		SNP1		
					SNP1-2		2.172	0.338
0.128	0.140	1.114	0.315	0.575		SNP2		
0.392	0.412	1.087	0.390	0.532				
0.468	0.510	1.184	1.630	0.202				
0.381	0.371	1.045	0.107	0.744		SNP5		
					SNP5-6		0.407	0.816
0.223	0.201	1.135	0.620	0.431		SNP6		
0.248	0.214	1.212	1.472	0.225				
0.115	0.148	1.336	2.001	0.157		SNP83		
0.000	0.000							
					SNP83-VNTR		21.389	0.002
0.468	0.436	1.137	0.939	0.333		SNP8		
0.335	0.396	1.298	3.348	0.067		VNTR		
0.055	0.061	1.117	0.156	0.693				
0.051	0.061	1.203	0.421	0.516		SNP10		
0.055	0.060	1.103	0.123	0.726				
					SNP9-13		0.640	0.726
0.055	0.061	1.122	0.167	0.683				
0.231	0.212	1.116	0.474	0.491		SNP13		
0.492	0.498	1.021	0.024	0.877		SNP14		
0.383	0.400	1.076	0.297	0.586				
					SNP14-17		0.274	0.965
0.367	0.379	1.053	0.148	0.700		SNP16		
0.362	0.355	1.028	0.040	0.841				
			5.594	0.588				
0.204	0.249	1.294	2.668	0.102	SNP18-22	SNP18		

(Continued)

TABLE 2. (Continued)

Variants			Gene Symbols	Position in Build 35.1	Distances Between Markers
Public ID	Celera ID				
rs3756739	C_3076518_10	SNP19	FLJ36754;SDCCAG10	64 100 167	
					14 604
rs6875372	C_1699198_10	SNP20	SDCCAG10	64 114 771	
					375 168
rs1423351	C_2836805_10	SNP21	ADAMTS6	64 489 939	
					143 176
rs10042323	C_1186571_10	SNP22	ADAMTS6	64 633 115	
					181 654
rs33395	C_1001782_10	SNP23	ADAMTS6	64 814 769	
					35 579
rs706657	C_1135885_10	SNP24	FKSG14	64 850 348	
					62 399
rs37338	C_3166401_10	SNP25	ARFD1	64 912 747	
					15 948
rs154854	C_3166346_1_	SNP26	ARFD1	64 955 747	
					94 844
rs2548788	C_7571886_10	SNP27	NLN	65 050 591	
					106 533
rs3733657	C_2145723_1_	SNP28	NLN	65 157 124	
					195 813
rs706679	C_7571528_10	SNP29	ERBB2IP	65 352 937	
					930 196
D5S647			K1AA0303	66 283 133	

date. If indeed the susceptibility genes or polymorphisms can be completely elucidated, these results will have a considerable impact on the medical community because stroke is one of the major public health concerns in the world today. With this goal in mind, we began our initial experiments in 2002. After Gretarsdottir et al further identified the *PDE4D* gene as a susceptibility gene for this locus in 2003,[4] we decided to attempt to confirm whether this *PDE4D* gene was also a susceptibility gene in Japanese subjects.

TABLE 3. Individual Haplotype Frequencies in the Haplotype Block Consisting of SNP83, 8, and VNTR

Haplotype	Non-Cerebral Infarction	Cerebral Infarction	χ^2	*P* Value
T-g-X	0.325	0.242	6.946	0.008*
T-A-X	0.261	0.255	0.030	0.863
T-A-0	0.189	0.238	2.949	0.086
T-g-0	0.116	0.119	0.012	0.912
c-A-X	0.076	0.075	0.004	0.953
c-g-0	0.032	0.041	0.473	0.492
c-g-X	0.000	0.030	13.809	0.000*

First character: alleles of SNP83. Large and small characters show the major and the minor alleles, respectively. 0 is an at-risk allele of VNTR, and X is a composite allele denoting all alleles of VNTR except allele 0.[4]
*Significant difference.

Candidate polymorphisms that were possible major risk factors for myocardial infarction in Japanese subjects were identified previously in a large-scale case-control study that used 92 788 gene-based SNP markers from the entire human genome.[25] The results of this study confirmed the value of whole genome scanning using SNPs for the identification of suscepti-

TABLE 4. Individual Haplotype Frequencies in the Haplotype Block Consisting of SNPs18, 19, 20, and 21

Haplotype	Non-Cerebral Infarction	Cerebral Infarction	χ^2	*P* Value
C-C-A-A	0.286	0.224	4.331	0.037*
C-g-A-g	0.208	0.200	0.082	0.775
C-C-A-g	0.096	0.115	0.878	0.349
C-g-A-A	0.087	0.088	0.004	0.948
C-g-t-g	0.080	0.040	5.242	0.022*
t-C-A-A	0.065	0.089	1.662	0.197
t-C-A-g	0.065	0.052	0.697	0.404
C-g-t-A	0.043	0.088	7.433	0.006*
t-g-A-g	0.036	0.063	3.470	0.063
t-g-A-A	0.034	0.021	1.325	0.250
t-g-t-g	0.000	0.020	10.596	0.001*

Large and small characters show major and minor alleles, respectively.
*Significant difference.

TABLE 2. (Continued)

Minor Allele Frequency		Odds Ratio At-Risk Allele	Allele		Haplotype			
Non-Cerebral Infarction	Cerebral Infarction	Cerebral Infarction	χ^2	*P* Value	Block	Tagged SNPs	χ^2	*P* Value
0.481	0.519	1.014	0.905	0.342		SNP19		
0.131	0.159	1.255	1.480	0.224		SNP20		
					SNP18-22		33.214	<0.001
0.492	0.483	1.039	0.083	0.773		SNP21		
0.445	0.420	1.108	0.597	0.440				
0.406	0.382	1.107	0.554	0.457				
0.340	0.306	1.170	1.252	0.263		SNP24		
0.408	0.387	1.090	0.410	0.522				
					SNP23-28		8.311	0.306
0.409	0.384	1.112	0.625	0.429				
0.299	0.328	1.141	0.872	0.351		SNP27		
0.192	0.223	1.205	1.320	0.251		SNP28		
0.443	0.432	1.047	0.121	0.728				
			7.363	0.691				

List of microsatellites and SNPs and their location on chromosome 5q.
D5S407 is located on the centromere side on 5q. D5S647 is on the telomere side on 5q.
The positions of SNPs and microsatellites are given the format of NCBJ Build 35.1.
Gray shading indicates the haplotype blocks and tagged SNPs.

bility genes of multifactorial diseases. Therefore, we designed a case-control study using SNPs and microsatellites in the susceptibility locus. In our study, the cerebral infarction patients and control subjects were selected based on considerably stricter criteria than those used in the Gretarsdottir et al study by excluding transient ischemic attack. To do this, cerebral infarction was defined as noncardiogenic ischemic stroke with signs and symptoms lasting >1 month in duration. Inclusion of the various subtypes of stroke may have increased the false-negative results in their case-control study.

Very recently, 2 groups independently reported that the *PDE4D* gene was not associated with stroke.[26,27] Not surprisingly, comparison of different studies produces different results,[28] and one explanation for these disparities is that different analytical methods, genetic maps, and markers are used. Furthermore, striking differences in incidence, prevalence, and the clinical patterns among different ethnic populations reported in several epidemiological studies support this view.

Our results suggest that there may be a susceptibility region other than that of the *PDE4D* gene within the locus in Japanese subjects. The region of the *PDE4D* gene may be the susceptibility region for cardioembolic stroke, whereas the region that we identified may be the susceptibility region for noncardiogenic ischemic stroke. Further studies are needed to isolate other susceptibility genes and determine the confounding between these 2 regions.

Acknowledgments

This work was supported by a grant from the Ministry of Education, Science and Culture of Japan (High-Tech Research Center, Nihon University) and a research grant from the Alumni Association of Nihon University School of Medicine. We would like to thank K. Sugama for her technical assistance.

References

1. Hassan A, Markus HS. Genetics and ischemic stroke. *Brain.* 2000;123: 1784–1812.
2. Kiely DK, Wolf PA, Cupples LA, Beiser AS, Myers RH. Familial aggregation of stroke. The Framingham Study. *Stroke.* 1993;24:1366–1371.
3. Gretarsdottir S, Sveinbjornsdottir S, Jonsson HH, Jakobsson F, Einarsdottir E, Agnarsson U, Shkolny D, Einarsson G, Gudjonsdottir HM, Valdimarsson EM, Einarsson OB, Thorgeirsson G, Hadzic R, Jonsdottir S, Reynisdottir ST, Bjarnadottir SM, Gudmundsdottir T, Gudlaugsdottir GJ, Gill R, Lindpaintner K, Sainz J, Hannesson HH, Sigurdsson GT,

Frigge ML, Kong A, Gudnason V, Stefansson K, Gulcher JR. Localization of a susceptibility gene for common forms of stroke to 5q12. *Am J Hum Genet.* 2002;70:593–603.
4. Gretarsdottir S, Thorleifsson G, Reynisdottir ST, Manolescu A, Jonsdottir S, Jonsdottir T, Gudmundsdottir T, Bjarnadottir SM, Einarsson OB, Gudjonsdottir HM, Hawkins M, Gudmundsson G, Gudmundsdottir H, Andrason H, Gudmundsdottir AS, Sigurdardottir M, Chou TT, Nahmias J, Goss S, Sveinbjornsdottir S, Valdimarsson EM, Jakobsson F, Agnarsson U, Gudnason V, Thorgeirsson G, Fingerle J, Gurney M, Gudbjartsson D, Frigge ML, Kong A, Stefansson K, Gulcher JR. The gene encoding phosphodiesterase 4D confers risk of ischemic stroke. *Nat Genet.* 2003;35:131–138.
5. Rahmutula D, Nakayama T, Soma M, Takahashi Y, Kunimoto M, Uwabo J, Sato M, Izumi Y, Kanmatsuse K, Ozawa Y. Association study between the variants of the human ANP Gene and essential hypertension. *Hypertens Res.* 2001;24:291–294.
6. Nakayama T, Soma M, Saito S, Honye J, Sato M, Aoi N, Kosuge K, Haketa A, Kanmatsuse K, Kokubun S. Missense mutation of exon 3 in the type A human natriuretic peptide receptor gene is associated with myocardial infarction. *Med Sci Monit.* 2003;9:CR505–CR510.
7. Hasimu B, Nakayama T, Mizutani Y, Izumi Y, Asai S, Soma M, Kokubun S, Ozawa Y. A novel variable number of tandem repeat polymorphism of the renin gene and essential hypertension. *Hypertens Res.* 2003;26:473–477.
8. Nakayama T, Soma M, Mizutani Y, X Xu, Honye J, Kaneko Y, Rahmutula D, Aoi N, Kosuge K, Saito S, Ozawa Y, Kanmatsuse K, Kokubun S. A novel missense mutation of exon 3 in the type A human natriuretic peptide receptor gene: possible association with essential hypertension. *Hypertens Res.* 2002;25:395–401.
9. Nakayama T, Soma M, Rahmutula D, Ozawa Y, Kanmatsuse K. Isolation of the 5′-flanking region of genes by thermal asymmetric interlaced polymerase chain reaction. *Med Sci Monit.* 2001;7:345–349.
10. Nakayama T, Soma M, Kanmatsuse K, Kokubun S. The microsatellite alleles on chromosome 1 associated with essential hypertension and blood pressure levels. *J Hum Hypertens.* 2004;18:823–828.
11. Sano M, Kuroi N, Nakayama T, Sato N, Izumi Y, Soma M, Kokubun S. The association study of calcitonin-receptor-like receptor gene in essential hypertension. *Am J Hypertens.* 2005;18:403–408.
12. Dempster AP, Laird NM, Rubin DB. Maximum likelihood from incomplete data via the EM algorithm. *J R Stat Soc.* 1977;39:1–22.
13. Kobayashi Y, Nakayama T, Sato N, Izumi Y, Kokubun S, Soma M. Haplotype-based case-control study revealing an association between the adrenomedullin gene and proteinuria in subjects with essential hypertension. *Hypertens Res.* 2005;28:229–236.
14. Einot I, Gabriel KR. A study of the powers of several methods of multiple comparisons. *J Am Stat Assoc.* 1975;70:574–583.
15. Nakayama T, Soma M, Takahashi Y, Izumi Y, Kanmatsuse K, Esumi M. Association analysis of CA repeat polymorphism of the endothelial nitric oxide synthase gene with essential hypertension in Japanese. *Clin Genet.* 1977;51:26–30.
16. Excoffier L, Slatkin M. Maximum-likelihood estimation of molecular haplotype frequencies in a diploid population. *Mol Biol Evol.* 1995;12:921–927.
17. Fallin D, Cohen A, Essioux L, Chumakov I, Blumenfeld M, Cohen D, Schork NJ. Genetic analysis of case/control data using estimated haplotype frequencies: application to APOE locus variation and Alzheimer's disease. *Genome Res.* 2001;11:143–151.
18. Johnson GC, Esposito L, Barratt BJ, Smith AN, Heward J, Di Genova G, Ueda H, Cordell HJ, Eaves IA, Dudbridge F, Twells RC, Payne F, Hughes W, Nutland S, Stevens H, Carr P, Tuomilehto-Wolf E, Tuomilehto J, Gough SC, Clayton DG, Todd JA. Haplotype tagging for the identification of common disease genes. *Nat Genet.* 2001;29:233–237.
19. Epstein MP, Satten GA. Inference on haplotype effects in case-control studies using unphased genotype data. *Am J Hum Genet.* 2003;73:1316–1329.
20. Kostulas K, Huang WX, Crisby M, Jin YP, He B, Lannfelt L, Eggertsen G, Kostulas V, Hillert J. An angiotensin-converting enzyme gene polymorphism suggests a genetic distinction between ischaemic stroke and carotid stenosis. *Eur J Clin Invest.* 1999;29:478–483.
21. Markus HS, Ruigrok Y, Ali N, Powell JF. Endothelial nitric oxide synthase exon 7 polymorphism, ischemic cerebrovascular disease, and carotid atheroma. *Stroke.* 1998;29:1908–1911.
22. Couderc R, Mahieux F, Bailleul S, Fenelon G, Mary R, Fermanian J. Prevalence of apolipoprotein E phenotypes in ischemic cerebrovascular disease. A case-control study. *Stroke.* 1993;24:661–664.
23. Reuner KH, Ruf A, Grau A, Rickmann H, Stolz E, Juttler E, Druschky K. Prothrombin gene G20210–>A transition is a risk factor for cerebral venous thrombosis. *Stroke.* 1998;29:765–769.
24. Markus HS, Ali N, Swaminathan R, Sankaralingam A, Molloy J, Powell J. A common polymorphism in the methylenetetrahydrofolate reductase gene, homocysteine, and ischemic cerebrovascular disease. *Stroke.* 1997; 28:1739–1743.
25. Ozaki K, Ohnishi Y, Iida A, Sekine A, Yamada R, Tsunoda T, Sato H, Sato H, Hori M, Nakamura Y, Tanaka T. Functional SNPs in the lymphotoxin-alpha gene that are associated with susceptibility to myocardial infarction. *Nat Genet.* 2002;32:650–654.
26. Lohmussaar E, Gschwendtner A, Mueller JC, Org T, Wichmann E, Hamann G, Meitinger T, Dichgans M. ALOX5AP gene and the PDE4D gene in a central European population of stroke patients. *Stroke.* 2005;36:731–736.
27. Bevan S, Porteous L, Sitzer M, Markus HS. Phosphodiesterase 4D gene, ischemic stroke, and asymptomatic carotid atherosclerosis. *Stroke.* 2005;36:949–753.
28. Nakayama T. Issues and progress in isolation of susceptibility genes of essential hypertension. *Curr Hypertens Rev.* 2002;1:77–87.

Activator Protein-1 Mediates Shear Stress–Induced Prostaglandin D Synthase Gene Expression in Vascular Endothelial Cells

Megumi Miyagi, Yoshikazu Miwa, Fumi Takahashi-Yanaga, Sachio Morimoto, Toshiyuki Sasaguri

Objective—We attempted to determine the molecular mechanism of fluid shear stress–induced lipocalin-type prostaglandin D synthase (L-PGDS) expression in vascular endothelial cells.

Methods and Results—We examined the promoter region of the L-PGDS gene by loading laminar shear stress (20 dyne/cm^2), using a parallel-plate flow chamber, on endothelial cells transfected with luciferase reporter vectors containing the 5′-flanking regions of the human L-PGDS gene. A deletion mutant analysis revealed that a shear stress–responsive element resided in the region between −2607 and −2523 bp. A mutation introduced into the putative binding site for activator protein-1 (AP-1) within this region eliminated the response to shear stress. In an electrophoretic mobility shift assay, shear stress stimulated nuclear protein binding to the AP-1 binding site, which was supershifted by antibodies to c-Fos and c-Jun. Shear stress elevated the c-Jun phosphorylation level in a time-dependent manner, similar to that of L-PGDS gene expression. SP600125, a c-Jun N-terminal kinase inhibitor, decreased the c-Jun phosphorylation, DNA binding of AP-1, and L-PGDS expression induced by shear stress. Additionally, an mRNA chase experiment using actinomycin D demonstrated that shear stress did not stabilize L-PGDS mRNA.

Conclusions—Shear stress induces L-PGDS expression by transcriptional activation through the AP-1 binding site. (*Arterioscler Thromb Vasc Biol.* 2005;25:970-975.)

Key Words: shear stress ■ vascular endothelial cells ■ PGD synthase ■ AP-1 ■ JNK

In vascular cells and tissues, prostaglandin D_2 (PGD_2) applied in vitro prevents platelet aggregation[1] and induces endothelium-dependent arterial relaxation.[2] PGD_2 is metabolized to the PGJ_2 family, which includes PGJ_2, Δ^{12}-PGJ_2, and 15-deoxy-$\Delta^{12,14}$-PGJ_2 (15d-PGJ_2), without the requirement of specific enzymes.[3] The PGJ_2 family, particularly 15d-PGJ_2, exhibits strong anti-inflammatory effects by inhibiting nuclear factor κB[4] and IκB kinase[5] or through the activation of a peroxisome proliferator-activated receptor-γ.[6] In macrophages, 15d-PGJ_2 inhibits inflammatory cytokine production, metalloproteinase-9 activation, and inducible NO synthase expression.[7,8] The PGJ_2 family strongly inhibits vascular smooth muscle cell proliferation and promotes smooth muscle cell differentiation.[9–11] In vascular endothelial cells, 15d-PGJ_2 inhibits apoptotic cell death by upregulating the caspase inhibitor cellular inhibitor of apoptosis protein 1 (c-IAP1).[12] The majority of the effects induced by PGD_2 and the PGJ_2 family members appear to be anti-inflammatory, and therefore atheroprotective, because atherosclerosis is considered to be a chronic inflammation in vascular cells and tissues.[13]

Lipocalin-type PGD synthase (L-PGDS) catalyzes the isomeric conversion of PGH_2 to PGD_2.[14] In human cardiovascular tissues, the L-PGDS mRNA is most strongly expressed in the heart, where immunoreactivity of the enzyme is localized in the myocardial and endocardial cells.[15] Human aortic endothelial cells and intimal smooth muscle cells in vivo also stain positive for the L-PGDS mRNA by in situ hybridization.[16] Recent studies have suggested relationships between L-PGDS and cardiovascular diseases. For example, L-PGDS is secreted into the coronary circulation in angina patients.[15] Elevated serum L-PGDS levels after coronary angioplasty correlate with a decreased occurrence of restenosis.[17] The L-PGDS expression levels in macrophages of human atherosclerotic plaques correlate with plaque stability.[18] Serum and urinary levels of L-PGDS are significantly elevated in patients with essential hypertension or renal dysfunction.[19] Therefore, increased L-PGDS levels in vivo may play a protective role in cardiovascular diseases and may also serve as a sensitive disease marker.

We reported previously that endothelial cells cultured under static conditions express very low amounts of L-PGDS, whereas the L-PGDS mRNA expression is markedly increased when loaded with arterial levels of laminar fluid shear stress.[16] However, the mechanism of the shear stress–induced L-PGDS gene expression remains to be determined.

Original received August 18, 2004; final version accepted January 25, 2005.

From the Department of Clinical Pharmacology (M.M., Y.M., F.T.-Y., S.M., T.S.), Graduate School of Medical Sciences, Kyushu University, Fukuoka, Japan; and Third Department of Internal Medicine (M.M.), University of the Ryukyus School of Medicine, Okinawa, Japan.

Correspondence to Toshiyuki Sasaguri, MD, PhD, Department of Clinical Pharmacology, Graduate School of Medical Sciences, Kyushu University, 3-1-1 Maidashi, Higashi-ku, Fukuoka 812-8582, Japan. E-mail sasaguri@med.kyushu-u.ac.jp

Arterioscler Thromb Vasc Biol. is available at http://www.atvbaha.org

DOI: 10.1161/01.ATV.0000159702.68591.0d

In the present study, we investigated the molecular mechanism of the shear stress–induced L-PGDS expression in vascular endothelial cells. We report that the L-PGDS expression induced by shear stress is mediated by activator protein-1 (AP-1) binding to the 5′-flanking region of the L-PGDS gene.

Materials and Methods

Chemicals

SP600125, a specific c-Jun N-terminal kinase (JNK) inhibitor, was purchased from Biomol Research Laboratories.

Cell Culture

Human umbilical vein endothelial cells (HUVECs) were isolated and cultured as described previously.[20] Bovine arterial endothelial cells (BAECs) were grown in DMEM supplemented with 10% FBS, 100 U/mL penicillin G, and 100 μg/mL streptomycin.

Shear Stress Apparatus

A confluent monolayer of endothelial cells on a polyester sheet (Plastic Suppliers) was placed in a parallel-plate flow chamber and subjected to steady laminar shear stress as described previously.[21]

Western Blot Analysis

Western blot analysis was performed as described previously[22] using the polyclonal anti–phospho-c-Jun antibody (Cell Signaling Technology), the polyclonal anti–c-Jun antibody (Santa Cruz Biotechnology), the polyclonal anti–c-Fos antibody (Santa Cruz Biotechnology), and the polyclonal anti–L-PGDS antibody (Maruha Corporation).

Luciferase Reporter Assay

The 5′-flanking regions of the human L-PGDS gene (−2707/+41, −2660/+41, −2607/+41, −2523/+41, −2426/+41, −2092/+41, −1574/+41, −1148/+41, and −681/+41bp; GenBank accession No. M98537) were amplified by polymerase chain reaction (PCR) from genomic DNA obtained from HUVECs and subcloned into the *SacI–XhoI* site of PGV-B3 (Toyo Ink Manufacturing Co.), a firefly luciferase reporter vector. The structure of the DNA constructs was verified by sequence analysis. Plasmid DNA (3 μg) and pRL-SV40 (0.03 μg), a *Renilla* luciferase expression vector (Toyo Ink Manufacturing Co.), were mixed with DMEM (250 μL); 10 μL Trans IT transfection reagent (Mirus Corporation) was added, and the mixture was incubated at room temperature for 15 minutes. The DNA/reagent mixture was added to 5.0×10^5 BAECs (50% to 70% confluence) grown on a 37×75 mm polyester sheet in DMEM containing 10% FBS. After transfection for 4 to 8 hours, cells were cultured overnight in fresh DMEM containing 10% FBS and subsequently placed in a flow chamber. Luciferase activities were measured using a double luciferase assay system (Toyo Ink Manufacturing Co.) and a luminometer Lumat LB9507 (Berthold Technologies). Firefly luciferase activities were normalized to those of *Renilla* luciferase.

Site-Directed Mutagenesis

Site-directed mutagenesis was performed using a QuickChange Site-Directed Mutagenesis Kit (Stratagene), as instructed by the manufacturer. The luciferase reporter construct containing the −2707/+41 region of the L-PGDS promoter was used as the DNA template. The mutations introduced into the putative binding sites for AP-1 (−2530/−2522, GTGACTCAA→GCTCGAGCA), AP-1 (−2203/−2195, ATGAATCAG→ACTCGAGCG), AP-1 (−1830/−1820, GGTGCTCGAGG→GGTGACCCAGG), thyroid hormone receptor (TR; TGGCCTTGGTGACCT→TGGAATTGGTGATTT), and GATA-1/2 (GGGGATGGCC→GGGTACCTCC) were verified by sequence analysis.

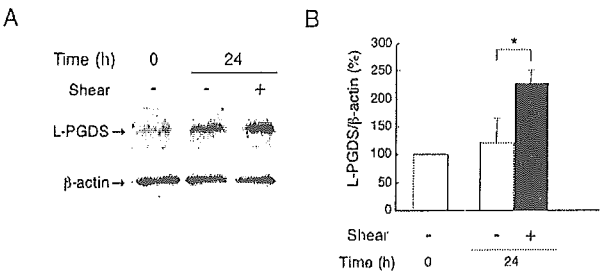

Figure 1. Effect of shear stress on L-PGDS protein expression. A, Confluent HUVECs were cultured under static conditions or exposed to shear stress (20 dyne/cm²) for 24 hours. L-PGDS expression was analyzed by Western blotting. A representative result from 3 independent experiments is shown. B, Data obtained in A was quantified. The L-PGDS expression levels normalized to those of β-actin are shown as percentages of the value obtained at time 0. *$P<0.05$ vs static control.

Electrophoretic Mobility Shift Assay

Nuclear proteins were extracted from HUVECs cultured on a 37×75 mm polyester sheet using NE-PER Nuclear and Cytoplasmic Extraction Reagents (Pierce). A double-stranded oligonucleotide probe containing the putative AP-1 binding site (5′-TTTGTGACTCAAAGAGACTG-3′) or its mutant (5′-TTTGCTCGAGCAAGAGACTG-3′) was labeled at the 3′-end with biotin using the Biotin 3′End DNA Labeling Kit (Pierce), as instructed by the manufacturer. Incubation for the DNA binding reaction was performed using the Lightshift Chemiluminescent EMSA (electrophoretic mobility shift assay) Kit (Pierce). A 100- to 200-fold molar excess of the unlabeled oligonucleotide was simultaneously added as a competitor, with the labeled probe. To identify DNA binding proteins, nuclear extracts were incubated with 3 μg of antibodies to c-Jun, c-Fos (Santa Cruz Biotechnology), or rabbit IgG at room temperature for 20 minutes, before the addition of the labeled probe. Anti-rabbit IgG was used as an irrelevant control. Protein–DNA complexes were electrophoresed on a 6% native polyacrylamide gel in buffer containing 45 mmol/L Tris, 45 mmol/L boric acid, and 1 mmol/L EDTA, pH 8.3, at 4°C. After transferring the samples to a positively charged nylon membrane using a semidry transfer system, the membrane was cross-linked at 100 mJ/cm². The biotin-labeled DNA was detected by the Lightshift Chemiluminescent EMSA Kit (Pierce) according to manufacturer protocol. A charge-coupled device camera (FluorChem; ASTEC) was used to detect chemiluminescence on the membrane.

Reverse Transcription–PCR

Total cellular RNA was extracted with Isogen (Nippon Gene). Using 1 μg of this RNA, the L-PGDS mRNA expression was analyzed by RT-PCR using the Ready-To-Go RT-PCR Beads (Amersham Biosciences),[16,23] and PCR primers were synthesized on the basis of the information obtained from the GenBank database.

Statistical Analysis

The results are expressed as mean±SE. Statistical significance was assessed by Student's *t* test.

Results

Vascular Endothelial Cells Express L-PGDS in Response to Shear Stress

Exposure to arterial levels (15 to 30 dyne/cm²) of laminar fluid shear stress markedly elevates the L-PGDS gene expression in HUVECs.[16] Using an antibody specific to L-PGDS, we examined the effect of shear stress on L-PGDS protein expression. As demonstrated in Figure 1, shear stress (20 dyne/cm²) loaded for 24 hours elevated the L-PGDS protein

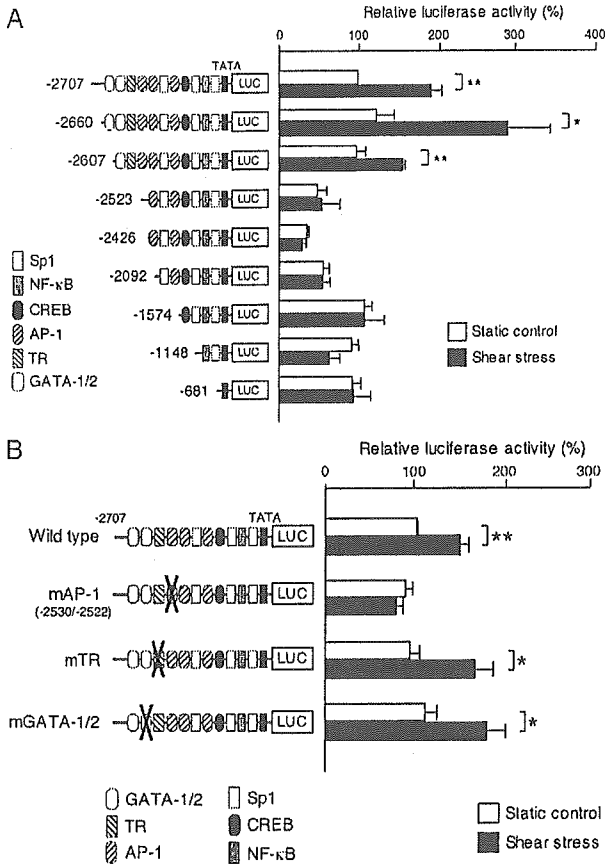

Figure 2. Analysis of the 5′-flanking region of the L-PGDS gene. A, PGV-B3, a firefly luciferase reporter vector containing various lengths of the 5′-flanking region of the L-PGDS gene, and pRL-SV40 were cotransfected into BAECs. Cells were then exposed to shear stress (20 dyne/cm^2) or maintained under static conditions for 24 hours. The firefly luciferase activities are shown as percentages of the value obtained in cells transfected with the plasmid containing the −2707/+41 region and cultured under static conditions. Error bars represent the SE values obtained from 3 or 4 independent experiments. *$P<0.05$; **$P<0.01$ vs static control. NF-κB indicates nuclear factor κB. B, The luciferase activities were compared between the wild-type and mutated constructs.

expression level by 1.9-fold compared with the static control. This result was consistent with the effect on the mRNA.

Analysis of the 5′-Flanking Region of the L-PGDS Gene

We attempted to determine the precise mechanism of the shear stress–induced L-PGDS expression by analyzing the L-PGDS gene promoter (Figure 2A; also see Figure I, available online at http://atvb.ahajournals.org). Luciferase reporter constructs driven by the 5′-flanking regions of the human L-PGDS gene (−2707/+41, −2660/+41, −2607/+41, −2523/+41, −2426/+41, −2092/+41, −1574/+41, −1148/+41, and −681/+41 bp) were transfected into BAECs. The promoter activities were measured after exposure to laminar shear stress (20 dyne/cm^2) for 24 hours because L-PGDS mRNA was maximally upregulated at 24 hours after the initiation of shear stress loading.[16] The reason for using BAECs in this experiment was that the efficiency of DNA transfection was much higher in BAECs (60% to 70%) than in HUVECs (10% to 20%). Shear stress induced 1.9-, 2.9-, and 1.6-fold increases in luciferase activity on transfection of the −2707/+41, −2660/+41, and −2607/+41 bp constructs, respectively. However, shear stress did not increase the activity when the −2523/+41 bp construct was used. Therefore, it is possible that the response element to shear stress was located between −2607 and −2523 bp in the 5′-flanking region, where the putative binding sites for GATA-1/2 (−2580/−2571), TR (−2575/−2561),[24] and AP-1 (−2530/−2522) are located.

Identification of the Shear Stress–Responsive Element

To identify the shear stress–responsive element residing between −2607 and −2523 bp of the L-PGDS gene, we introduced mutations into the 3 putative binding sites (GATA-1/2, TR, and AP-1) to destroy the consensus sequences, as described in Materials and Methods. The mutations in the consensus sequences for GATA-1/2 (−2580/−2571) or TR (−2575/−2561) had no effect on the shear stress response (Figure 2B). In contrast, the mutation introduced into the putative AP-1 binding site (−2530/−2522) completely eliminated the response to shear stress, suggesting the possibility that this site is involved in the response.

In addition, destruction of the proximal AP-1 consensus sites (−2203/−2195 and −1830/−1820) had no effect on the response (Figure II, available online at http://atvb.ahajournals.org).

Shear Stress Stimulates AP-1 Binding to the L-PGDS Gene

We attempted to identify the transcription factor involved in the shear stress–induced transactivation of the L-PGDS gene by EMSA using a DNA oligonucleotide containing the putative AP-1 binding site (−2532/−2513). Shear stress loaded on HUVECs for 24 hours stimulated the binding of a nuclear protein to the oligonucleotide (Figure 3A, lane 3). The addition of a 100- to 200-fold molar excess of the unlabeled oligonucleotide (wild type [WT]) resulted in a marked reduction of the shifted band (Figure 3A and 3B). In contrast, a mutant oligonucleotide (mAP-1), in which the same mutation as that used for the luciferase reporter assay was introduced, failed to compete for binding to AP-1 (Figure 3B, lane 4).

Subsequently, we examined the effect of anti–c-Jun and anti–c-Fos antibodies because the AP-1 complex may comprise either a c-Jun/c-Fos heterodimer or a c-Jun/c-Jun homodimer. Supershifted complexes were observed in the presence of the anti–c-Jun or anti–c-Fos antibodies (Figure 3C, lanes 2 and 3, top arrow). Therefore, the involvement of AP-1, at least in part including c-Jun/c-Fos heterodimers, was suggested in the shear stress–induced DNA–protein binding.

In addition, to investigate the involvement of JNK, we used its specific inhibitor SP600125. As shown in Figure 3D, SP600125 inhibited the DNA–protein complex formation, suggesting that the L-PGDS gene transcription is regulated by AP-1 through JNK activation.

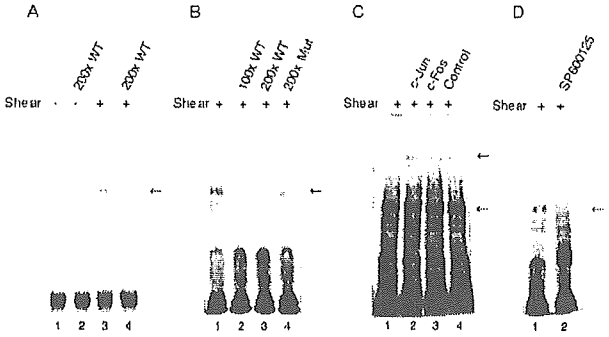

Figure 3. EMSA for the putative AP-1 binding site. A and B, Nuclear extracts (5 μg per lane) from HUVECs exposed to shear stress (20 dyne/cm²) for 24 hours were analyzed by EMSA using a double-stranded DNA oligonucleotide probe corresponding to the −2532/−2513 bp region of the L-PGDS gene. Extracts were incubated with 100- or 200-fold molar excess of the unlabeled probe (WT) or a mutant probe (Mut) as competitors, at room temperature for 20 minutes before the addition of the labeled probe. C, Supershift analyses were performed as described under Materials and Methods using the antibodies to c-Jun and c-Fos. D, Cells were stimulated by shear stress in the presence of SP600125 (20 μmol/L) for 24 hours. A representative result from 3 independent experiments is shown.

c-Jun Phosphorylation Induced by Shear Stress

To elucidate the mechanism by which shear stress stimulates AP-1 activation, we examined whether shear stress elevates the c-Jun or c-Fos expression levels or activates JNK, which activates c-Jun by phosphorylation. As shown in Figure 4A,

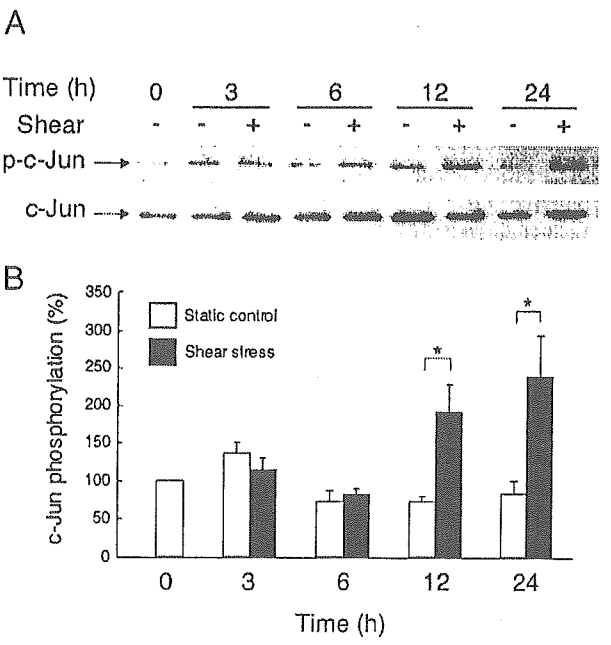

Figure 4. Effect of shear stress on c-Jun phosphorylation. A, Confluent HUVECs were cultured under static conditions or loaded with shear stress (20 dyne/cm²) for the periods indicated. The phosphorylated and total c-Jun protein levels were analyzed by Western blotting. B, Data obtained in A was quantified. The phosphorylated c-Jun protein expression levels normalized to those of total c-Jun are shown as percentages of the value obtained at time 0. Error bars represent the SE values obtained from 3 to 4 independent experiments. *$P<0.05$ vs static control.

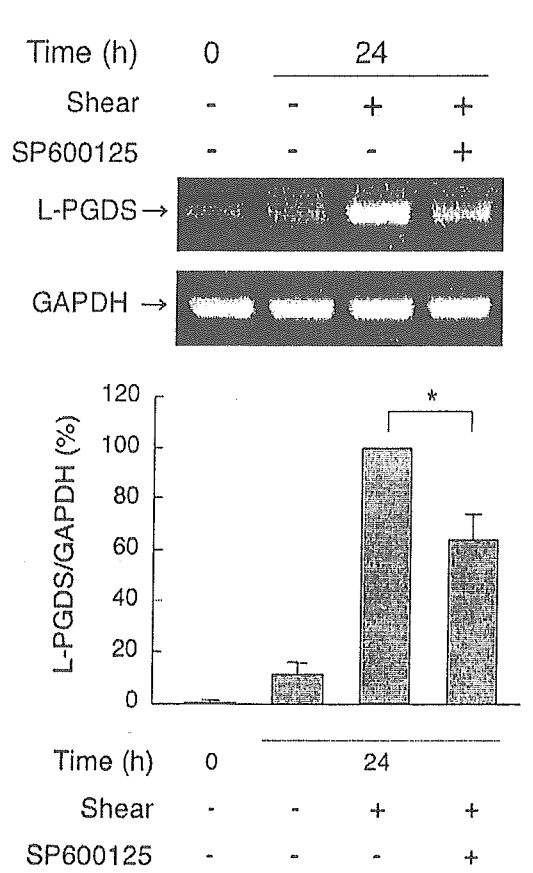

Figure 5. Effect of SP600125 on L-PGDS gene expression. HUVECs were cultured under shear stress (20 dyne/cm²) for 24 hours in the presence or absence of SP600125 (20 μmol/L). A, Total RNA (1 μg) was analyzed by RT-PCR for L-PGDS and GAPDH. B, Data obtained from 3 independent experiments were quantified. *$P<0.05$.

the c-Jun level was not increased by shear stress. However, the c-Jun phosphorylation level was slowly elevated by loading shear stress, and it was maximal at 24 hours (Figure 4A and 4B). Importantly, this time course was very similar to the time course of L-PGDS induction by shear stress.[15] On the other hand, c-Fos, the other component of AP-1, was persistently expressed, regardless of the loading shear stress (Figure III, available online at http://atvb.ahajournals.org).

c-Jun is phosphorylated by JNK. To investigate whether JNK mediates the shear stress–dependent L-PGDS induction, HUVECs were exposed to shear stress in the presence of SP600125. SP600125 significantly attenuated the shear stress–dependent c-Jun phosphorylation (Figure IV, available online at http://atvb.ahajournals.org) and L-PGDS mRNA induction (Figure 5), thereby suggesting the involvement of JNK.

Shear Stress Does Not Stabilize L-PGDS mRNA

To examine whether post-transcriptional mechanisms are involved in the shear stress–induced L-PGDS expression, we followed the decay of the L-PGDS mRNA after the addition of transcriptional inhibitor actinomycin D. The L-PGDS mRNA expressed in HUVECs pre-exposed to shear stress for 24 hours was slowly degraded after the cessation of shear

stress in the presence of actinomycin D (Figure V, available online at http://atvb.ahajournals.org). The degradation of the L-PGDS mRNA did not significantly slow down even when shear stress was continuously loaded after the addition of actinomycin D. Therefore, shear stress appeared to elevate the L-PGDS mRNA expression level by activating the transcription and not by stabilizing the mRNA.

Discussion

We reported previously that vascular endothelial cells express the L-PGDS mRNA in vitro and in vivo, and laminar shear stress stimulates its expression and PGD_2 production in vitro.[16] As first shown in this article, we confirmed that the L-PGDS protein expression level also increases in response to shear stress. However, the manner in which shear stress induces the L-PGDS gene expression was unknown. Therefore, we attempted to identify the mechanism by which shear stress stimulates the L-PGDS mRNA expression. Consequently, we found that AP-1 mediates the shear stress–induced L-PGDS expression. To our knowledge, this is the first report of a shear stress–responsive element in the human L-PGDS gene.

Although fluid shear stress is known to elevate the expression levels of some proteins by stabilizing their mRNAs, such as granulocyte–macrophage colony-stimulating factor,[25] cyclooxygenase-2,[26] and cyclin-dependent kinase inhibitor p21 (Miwa et al, unpublished data, 2004), shear stress did not prolong the half life of the L-PGDS mRNA. This suggests that shear stress stimulates transcription of the L-PGDS gene.

The deletion analysis of the 5′-flanking region of the L-PGDS gene indicated that the response to shear stress depended on the region between −2607 and −2523 bp, where the putative binding sites for GATA-1/2, TR, and AP-1 are located. Among these, only the TR consensus site has been reported to function in vitro and in vivo. The complex of T_3 and TR-β stimulates the L-PGDS promoter by binding to the thyroid hormone–responsive element in COS-7 cells[27] and human medulloblastoma TE671 cells.[24] The L-PGDS mRNA expression level decreases in the brain of hypothyroid rats.[28,29] However, in our study, deletion or mutation of the TR or GATA-1/2 consensus sites had no effect on the shear stress–induced increase in luciferase activity. Only the mutation introduced into the AP-1 binding site abolished the shear stress response. Although there are 2 other AP-1 consensus sites in the proximal region (−2203/−2195 and −1830/−1820), destruction of them had no influence on the shear stress response. Therefore, the distal AP-1 site (−2530/−2522), and not the TR, GATA-1/2, or proximal AP-1 sites, seemed to be required for the shear stress–induced L-PGDS gene expression. In addition, deleting the region between −2707 and −2660 bp, which did not contain any known consensus sequence, enhanced the shear stress response, suggesting the possibility of suppressor elements in this region.

The involvement of AP-1 was confirmed by the subsequently performed EMSA. Exposure to shear stress increased nuclear protein binding to the oligonucleotide, including the AP-1 consensus site, primarily identified as the 12-O-tetradecanoyl phorbol 13-acetate–responsive element (TRE).[30] The anti–c-Jun and anti–c-Fos antibodies partially supershifted the protein–DNA complex, suggesting that AP-1, at least in part, including c-Jun/c-Fos heterodimers, is involved in the response. The c-Jun/c-Fos heterodimers form more stable complexes with TRE, thereby exhibiting a stronger transactivation than the c-Jun/c-Jun homodimers.[31]

Previous studies have suggested the involvement of AP-1 in the shear stress–induced gene expression of some endothelial cell proteins, such as monocyte chemoattractant protein-1 (MCP-1)[32] and vascular cell adhesion molecule-1 (VCAM-1).[33] AP-1 upregulates the MCP-1 gene expression by stimulating TRE in the MCP-1 gene promoter.[32] On the other hand, AP-1 downregulates VCAM-1 through 2 consensus AP-1 binding sites.[33]

Shear stress has been reported to increase the amounts of c-Jun and c-Fos at the mRNA and the protein levels in human endothelial cells.[34,35] However, in this study, shear stress had no significant influence on c-Jun or c-Fos expression levels. AP-1 expression is induced by multiple stimuli, including serum and growth factors.[36] In this experiment, c-Fos and c-Jun proteins might have already been expressed at time 0 because HUVECs were cultured in DMEM supplemented with 20% FBS and basic fibroblast growth factor.

Phosphorylation is required for the activation of AP-1 family members. With regard to Jun proteins, the activation domain is regulated to a large extent by the JNK family of mitogen-activated protein kinases.[30] JNK phosphorylates c-Jun at Ser-63, resulting in the binding of c-Jun to the CREB-binding protein/p300 family of transcriptional coactivators.[30] Regarding Fos proteins, the N-terminal and C-terminal domains flanking the basic leucine zipper domain require phosphorylation for their biological activity. Kinases responsible for the phosphorylation of Fos proteins remain to be determined.[30,37] In the present study, the phosphorylation level of c-Jun was slowly but significantly elevated after loading shear stress. This finding is consistent with a previous report[38] that the shear stress–induced phosphorylation of c-Jun takes several hours to reach a maximal level. Furthermore, SP600125 inhibited the shear stress–induced DNA–protein complex formation and L-PGDS mRNA expression. Therefore, induction of the L-PGDS gene by shear stress appeared to be mediated by AP-1, which is activated on phosphorylation by JNK.

Vascular endothelium plays an essential role as a physiological barrier to protect vascular walls from undergoing atherosclerotic changes. The PGD_2 and PGJ_2 family, produced by endothelial cells in response to shear stress, might be involved in the endothelial cell functions. In particular, the PGJ_2 family members are unique in nature; they can strongly repress inflammatory processes and inhibit apoptosis in vascular endothelial cells. We hypothesize that the PGJ_2 family produced by endothelial cells maintains vascular homeostasis by functioning as an antiatherogenic factor, analogous to NO, PGI_2, and other endothelium-derived substances. Substances that modify PGD_2 metabolism might provide novel preventive and therapeutic strategies for the treatment of atherosclerotic vascular diseases.

In conclusion, our present study has demonstrated that AP-1 activated by c-Jun phosphorylation mediates the lami-

nar fluid shear stress–induced transcriptional activation of the human L-PGDS gene in vascular endothelial cells. Further study is required to elucidate the physiological and pathological roles of this mechanism.

Acknowledgements

This study was supported by a grant-in-aid for scientific research from the Ministry of Education, Culture, Sports, Science, and Technology, Japan. We thank Nobuyuki Sato, Yasuhiko Shiina, and Hiroshi Oda, Central Research Institute, and Maruha Corporation (Tokyo, Japan) for providing the anti-L-PGDS antibody. We also thank Hiroyasu Inoue, Department of Food Science and Nutrition, Nara Women's University (Nara, Japan), for providing BAECs and valuable discussions.

References

1. Bushfield M, McNicol A, MacIntyre DE. Inhibition of platelet-activating-factor-induced human platelet activation by prostaglandin D_2. Differential sensitivity of platelet transduction processes and functional responses to inhibition by cyclic AMP. *Biochem J.* 1985;232:267–271.
2. Braun M, Schrör K. Prostaglandin D_2 relaxes bovine coronary arteries by endothelium-dependent nitric oxide-mediated cGMP formation. *Circ Res.* 1992;71:1305–1313.
3. Fitzpatrick FA, Wynalda MA. Albumin-catalyzed metabolism of prostaglandin D_2. Identification of products formed in vitro. *J Biol Chem.* 1983;258:11713–11718.
4. Straus DS, Pascual G, Li M, Welch JS, Ricote M, Hsiang CH, Sengchanthalangsy LL, Ghosh G, Glass CK. 15-Deoxy-$\Delta^{12,14}$-prostaglandin J_2 inhibits multiple steps in the NF-κB signaling pathway. *Proc Natl Acad Sci U S A.* 2000;97:4844–4849.
5. Rossi A, Kapahi P, Natoli G, Takahashi T, Chen Y, Karin M, Santoro MG. Anti-inflammatory cyclopentenone prostaglandins are direct inhibitors of IκB kinase. *Nature.* 2000;403:103–108.
6. Ricote M, Li AC, Willson TM, Kelly CJ, Glass CK. The peroxisome proliferator-activated receptor-γ is a negative regulator of macrophage activation. *Nature.* 1998;391:79–82.
7. Straus DS, Glass CK. Cyclopentenone prostaglandins: new insights on biological activities and cellular targets. *Med Res Rev.* 2001;21:185–210.
8. Sasaguri T, Miwa Y. Prostaglandin J_2 family and the cardiovascular system. *Curr Vasc Pharmacol.* 2004;2:103–114.
9. Sasaguri T, Masuda J, Shimokado K, Yokota T, Kosaka C, Fujishima M, Ogata J. Prostaglandins A and J arrest the cell cycle of cultured vascular smooth muscle cells without suppression of c-myc expression. *Exp Cell Res.* 1992;200:351–357.
10. Miwa Y, Sasaguri T, Inoue H, Taba Y, Ishida A, Abumiya T. 15-Deoxy-$\Delta^{12,14}$-prostaglandin J_2 induces G_1 arrest and differentiation marker expression in vascular smooth muscle cells. *Mol Pharmacol.* 2000;58:837–844.
11. Miwa Y, Takahashi-Yanaga F, Morimoto S, Sasaguri T. Involvement of clusterin in 15-deoxy-$\Delta^{12,14}$-prostaglandin J_2-induced vascular smooth muscle cell differentiation. *Biochem Biophys Res Commun.* 2004;319:163–168.
12. Taba Y, Miyagi M, Miwa Y, Inoue H, Takahashi-Yanaga F, Morimoto S, Sasaguri T. 15-deoxy-$\Delta^{12,14}$-prostaglandin J_2 and laminar fluid shear stress stabilize c-IAP1 in vascular endothelial cells. *Am J Physiol Heart Circ Physiol.* 2003;285:H38–H46.
13. Ross R. Atherosclerosis–an inflammatory disease. *N Engl J Med.* 1999;340:115–126.
14. Urade Y, Hayaishi O. Prostaglandin D synthase: structure and function. *Vitam Horm.* 2000;58:89–120.
15. Eguchi Y, Eguchi N, Oda H, Seiki K, Kijima Y, Matsu-ura Y, Urade Y, Hayaishi O. Expression of lipocalin-type prostaglandin D synthase (β-trace) in human heart and its accumulation in the coronary circulation of angina patients. *Proc Natl Acad Sci U S A.* 1997;94:14689–14694.
16. Taba Y, Sasaguri T, Miyagi M, Abumiya T, Miwa Y, Ikeda T, Mitsumata M. Fluid shear stress induces lipocalin-type prostaglandin D_2 synthase expression in vascular endothelial cells. *Circ Res.* 2000;86:967–973.
17. Inoue T, Takayanagi K, Morooka S, Uehara Y, Oda H, Seiki K, Nakajima H, Urade Y. Serum prostaglandin D synthase level after coronary angioplasty may predict occurrence of restenosis. *Thromb Haemost.* 2001;85:165–170.
18. Cipollone F, Fazia M, Iezzi A, Ciabattoni G, Pini B, Cuccurullo C, Ucchino S, Spigonardo F, De Luca M, Prontera C, Chiarelli F, Cuccurullo F, Mezzetti A. Balance between PGD synthase and PGE synthase is a major determinant of atherosclerotic plaque instability in humans. *Arterioscler Thromb Vasc Biol.* 2004;24:1259–1265.
19. Hirawa N, Uehara Y, Yamakado M, Toya Y, Gomi T, Ikeda T, Eguchi Y, Takagi M, Oda H, Seiki K, Urade Y, Umemura S. Lipocalin-type prostaglandin D synthase in essential hypertension. *Hypertension.* 2002;39:449–454.
20. Kosaka C, Sasaguri T, Masuda J, Zen K, Shimokado K, Yokota T, Ogata J. Protein kinase C-mediated inhibition of cyclin A expression in human vascular endothelial cells. *Biochem Biophys Res Commun.* 1993;193:991–998.
21. Akimoto S, Mitsumata M, Sasaguri T, Yoshida Y. Laminar shear stress inhibits vascular endothelial cell proliferation by inducing cyclin-dependent kinase inhibitor $p21^{Sdi1/Cip1/Waf1}$. *Circ Res.* 2000;86:185–190.
22. Takahashi-Yanaga F, Taba Y, Miwa Y, Kubohara Y, Watanabe Y, Hirata M, Morimoto S, Sasaguri T. *Dictyostelium* differentiation-inducing factor-3 activates glycogen synthase kinase-3β and degrades cyclin D1 in mammalian cells. *J Biol Chem.* 2003;278:9663–9670.
23. Ishida A, Sasaguri T, Miwa Y, Kosaka C, Taba Y, Abumiya T. Tumor suppressor p53 but not cGMP mediates NO-induced expression of $p21^{Waf1/Cip1/Sdi1}$ in vascular smooth muscle cells. *Mol Pharmacol.* 1999;56:938–946.
24. White DM, Takeda T, DeGroot LJ, Stefansson K, Arnason BGW. β-Trace gene expression is regulated by a core promoter and a distal thyroid hormone response element. *J Biol Chem.* 1997;272:14387–14393.
25. Kosaki K, Ando J, Korenaga R, Kurokawa T, Kamiya A. Fluid shear stress increases the production of granulocyte-macrophage colony-stimulating factor by endothelial cells via mRNA stabilization. *Circ Res.* 1998;82:794–802.
26. Inoue H, Taba Y, Miwa Y, Yokota C, Miyagi M, Sasaguri T. Transcriptional and posttranscriptional regulation of cyclooxygenase-2 expression by fluid shear stress in vascular endothelial cells. *Arterioscler Thromb Vasc Biol.* 2002;22:1415–1420.
27. García-Fernández LF, Urade Y, Hayaishi O, Bernal J, Muñoz A. Identification of a thyroid hormone response element in the promoter region of the rat lipocalin-type prostaglandin D synthase (β-trace) gene. *Brain Res Mol Brain Res.* 1998;55:321–330.
28. García-Fernández LF, Iñiguez MA, Rodríguez-Peña A, Muñoz A, Bernal J. Brain-specific prostaglandin D_2 synthetase mRNA is dependent on thyroid hormone during rat brain development. *Biochem Biophys Res Commun.* 1993;196:396–401.
29. García-Fernández LF, Rausell E, Urade Y, Hayaishi O, Bernal J, Muñoz A. Hypothyroidism alters the expression of prostaglandin D2 synthase/β-trace in specific areas of the developing rat brain. *Eur J Neurosci.* 1997;9:1566–1573.
30. Karin M. The regulation of AP-1 activity by mitogen-activated protein kinases. *J Biol Chem.* 1995;270:16483–16486.
31. Halazonetis TD, Georgopoulos K, Greenberg ME, Leder P. c-Jun dimerizes with itself and with c-Fos, forming complexes of different DNA binding affinities. *Cell.* 1988;55:917–924.
32. Shyy JY, Lin MC, Han J, Lu Y, Petrime M, Chien S. The *cis*-acting phorbol ester "12-O-tetradecanoylphorbol 13-acetate"-responsive element is involved in shear stress-induced monocyte chemotactic protein 1 gene expression. *Proc Natl Acad Sci U S A.* 1995;92:8069–8073.
33. Korenaga R, Ando J, Kosaki K, Isshiki M, Takada Y, Kamiya A. Negative transcriptional regulation of the VCAM-1 gene by fluid shear stress in murine endothelial cells. *Am J Physiol.* 1997;273:C1506–C1515.
34. Lan Q, Mercurius KO, Davies PF. Stimulation of transcription factors NFκB and AP1 in endothelial cells subjected to shear stress. *Biochem Biophys Res Commun.* 1994;201:950–956.
35. Hsieh HJ, Li NQ, Frangos JA. Pulsatile and steady flow induces c-fos expression in human endothelial cells. *J Cell Physiol.* 1993;154:143–151.
36. Wisdom R. AP-1: one switch for many signals. *Exp Cell Res.* 1999;253:180–185.
37. Skinner M, Qu S, Moore C, Wisdom R. Transcriptional activation and transformation by FosB protein require phosphorylation of the carboxyl-terminal activation domain. *Mol Cell Biol.* 1997;17:2372–2380.
38. Jo H, Sipos K, Go YM, Law R, Rong J, McDonald JM. Differential effect of shear stress on extracellular signal-regulated kinase and N-terminal Jun kinase in endothelial cells. G_i2- and Gβ/γ-dependent signaling pathways. *J Biol Chem.* 1997;272:1395–1401.

Available online at www.sciencedirect.com
SCIENCE DIRECT®
Biochemical and Biophysical Research Communications 338 (2005) 903–909
BBRC
www.elsevier.com/locate/ybbrc

Differentiation-inducing factor-1 suppresses gene expression of cyclin D1 in tumor cells ☆

Tania Yasmin [a], Fumi Takahashi-Yanaga [a,*], Jun Mori [a], Yoshikazu Miwa [a], Masato Hirata [b], Yutaka Watanabe [c], Sachio Morimoto [a], Toshiyuki Sasaguri [a]

[a] *Department of Clinical Pharmacology, Graduate School of Medical Sciences, Kyushu University, Fukuoka 812-8582, Japan*
[b] *Department of Molecular and Cellular Biochemistry, Graduate School of Dental Sciences, Kyushu University, Fukuoka 812-8582, Japan*
[c] *Department of Applied Chemistry, Faculty of Engineering, Ehime University, Matsuyama 790-8577, Japan*

Received 5 October 2005
Available online 14 October 2005

Abstract

To determine the mechanism by which differentiation-inducing factor-1 (DIF-1), a morphogen of *Dictyostelium discoideum*, inhibits tumor cell proliferation, we examined the effect of DIF-1 on the gene expression of cyclin D1. DIF-1 strongly reduced the expression of cyclin D1 mRNA and correspondingly decreased the amount of β-catenin in HeLa cells and squamous cell carcinoma cells. DIF-1 activated glycogen synthase kinase-3β (GSK-3β) and inhibition of GSK-3β attenuated the DIF-1-induced β-catenin degradation, indicating the involvement of GSK-3β in this effect. Moreover, DIF-1 reduced the activities of T-cell factor (TCF)/lymphoid enhancer factor (LEF) reporter plasmid and a reporter gene driven by the human cyclin D1 promoter. Eliminating the TCF/LEF consensus site from the cyclin D1 promoter diminished the effect of DIF-1. These results suggest that DIF-1 inhibits Wnt/β-catenin signaling, resulting in the suppression of cyclin D1 promoter activity.

Keywords: Wnt signal; GSK-3β; β-Catenin; TCF/LEF; Cyclin D1; Differentiation-inducing factor; Gene expression; HeLa; Squamous cell carcinoma

Differentiation-inducing factor-1 (DIF-1) is a low molecular weight hydrophobic chemical substance (1-(3, 5-dichloro-2,6-dihydroxy-4-methoxyphenyl)-1-hex-anone) identified in *Dictyostelium discoideum* as a morphogen required for stalk cell differentiation [1,2]. However, the effect of the DIF family is not limited in *Dictyostelium*. DIF-1 and/or DIF-3, dechlorinated form of DIF-1, strongly inhibit cell proliferation and induce cell differentiation in several mammalian cells [3,4]. Although we reported that DIF-1 and DIF-3 suppressed the mRNA expression of cyclin D1 in vascular smooth muscle cells and HeLa cells [5,6], the precise mechanism underlying this effect is still unknown. As yet, the pharmacological target molecule for the DIF family substances has not been identified even in *Dictyostelium*.

Cyclin D1 is synthesized in the early G_1 phase and plays a key role in the initiation and progression of this phase. Genetic aberrations in the regulatory circuits that govern transit through the G_1 phase of the cell cycle occur frequently in human cancer. Overexpression of cyclin D1 is one of the most commonly observed alterations [7,8]. When cells enter the S phase, cyclin D1 is rapidly degraded by the ubiquitin-dependent mechanism, which requires the phosphorylation of threonine residues located near the carboxyl terminus. Glycogen synthase kinase-3β (GSK-3β), a member of the Wnt signaling pathway, is a kinase responsible for this phosphorylation [9–11]. Not only protein degradation, but also mRNA expression of cyclin D1 is

☆ *Abbreviations:* DIF-1,differentiation-inducing factor-1; GSK-3β, glycogen synthase kinase-3β; TCF, T-cell factor; LEF, lymphoid enhancer factor; FBS, fetal bovine serum; PAGE, polyacrylamide gel electrophoresis.

* Corresponding author. Fax: +81 92 642 6084.
E-mail address: yanaga@clipharm.med.kyushu-u.ac.jp (F. Takahashi-Yanaga).

0006-291X/$ - see front matter © 2005 Elsevier Inc. All rights reserved.
doi:10.1016/j.bbrc.2005.10.018

regulated by Wnt signaling pathway. The mRNA expression of cyclin D1 is regulated by β-catenin and GSK-3β also phosphorylates β-catenin to trigger the degradation. The Wnt signal inhibits GSK-3β and thereby induces the expression of β-catenin target genes through the activation of T-cell factor (TCF)/lymphoid enhancer factor (LEF), including cyclin D1 gene (CCND1) [12–16].

Therefore, in the present study, we tried to identify the mechanism for the DIF-1-induced suppression of cyclin D1 mRNA expression with regard to the involvement of GSK-3β, β-catenin, and TCF/LEF. We found that DIF-1 induces GSK-3β-mediated degradation of β-catenin, resulting in the suppression of TCF/LEF transcriptional activity in the cyclin D1 promoter.

Materials and methods

Chemicals and antibodies. DIF-1 (1-(3,5-dichloro-2,6-dihydroxy-4-methoxyphenyl)-1-hexanone) was synthesized according to Masento et al. [17]. *N*-Acetyl-Leu-Leu-norleucinal (ALLN) was purchased from Sigma. SB-216763 was from BIOMOL international. Wild-type cyclin D1 pGL3 basic luciferase reporter construct and its mutant were generous gifts from Drs. O. Tetsu and F. McCormick, University of California, San Francisco. TOPflash (TCF Reporter Plasmid) and FOPflash (negative control to TOPflash) were purchased from Upstate Biotechnology. The monoclonal anti-GSK-3β antibody and the monoclonal anti-β-catenin antibody were purchased from BD Transduction Laboratories. The polyclonal anti-phospho-GSK-3β (Ser^9) antibody was from Cell Signaling Technology. The polyclonal anti-cyclin D1 antibody was from Santa Cruz Biotechnology. The monoclonal anti-β-actin antibody was from Sigma. The monoclonal anti-α-tublin antibody was from Calbiochem.

Cell culture. Human cervical carcinoma cell line HeLa and human squamous cell carcinoma cell line NA [18] were grown in Dulbecco's modified Eagle's medium (Sigma) supplemented with 10% fetal bovine serum, 100 U/ml penicillin G, and 0.1 mg/ml streptomycin.

Immunoblotting. Immunoblotting was carried out as described previously [6]. Briefly, samples were separated by 12% SDS–polyacrylamide gel electrophoresis (SDS–PAGE) and transferred to a polyvinylidene difluoride membrane using a semi-dry transfer system (1 h, 15 V). After blocking with 5% skim milk for 1 h, the membrane was probed with a first antibody. The membrane was washed three times and incubated with horseradish peroxidase-conjugated anti-rabbit IgG or anti-mouse IgG (Bio-Rad) for 1 h. Immunoreactive proteins on the membrane were visualized by treatment with a detection reagent (LumiGLO, Cell Signaling Technology). An optical densitometric scan was performed using Science Lab 99 Image Gauge Software (Fuji Photo Film).

Northern blotting. Total cellular RNA was extracted with TRIzol Reagent (Invitrogen). Using 5 μg of the RNA, the expression of cyclin D1 was analyzed by Northern blotting as described previously [19,20].

Luciferase reporter assay. HeLa cells were transfected with luciferase reporter plasmids (TOPflash, FOPflash, wild-type cyclin D1 pGL3, or mutant cyclin D1 pGL3) and pRL-SV40, a *Renilla* luciferase expression plasmid (Toyo Ink Mfg), for the control of transfection efficiency, using Lipofect amine plus reagent (Invitrogen). Cells were cultured for 24 h after transfection and stimulated with DIF-1 (30 μM) for the periods indicated. The luciferase activity was determined with a luminometer (Lumat LB 9507, Berthold Technologies) and normalized with respect to *Renilla* luciferase activity.

Purification of nucleic proteins. Nucleic proteins were purified from cells cultured in 100-mm plates using NE-PER nuclear and cytoplasmic extraction reagents (PIERCE). Five micrograms of each sample was subjected to Western blot analysis.

Results

DIF-1 reduced the protein and mRNA expression levels of cyclin D1

We reported that DIF-1 reduces the expression of cyclin D1 and inhibits the cell cycle progression in vascular smooth muscle cells and squamous cell carcinoma cell lines [5,21]. Subsequently, we found that DIF-3 induces the rapid degradation of cyclin D1 protein and slow reduction in the expression level of cyclin D1 mRNA in HeLa cells [6]. First in the present study, we examined whether DIF-1 has the same effects as DIF-3 in HeLa cells. As shown in Figs. 1A and B, DIF-1 rapidly (within 1 h) decreased cyclin D1 protein in a time- and dose-dependent manner. Although DIF-1 also reduced the expression level of cyclin D1 mRNA, it took 6 h to significantly decrease the amount of the mRNA (Fig. 1C). These effects were unlikely to be

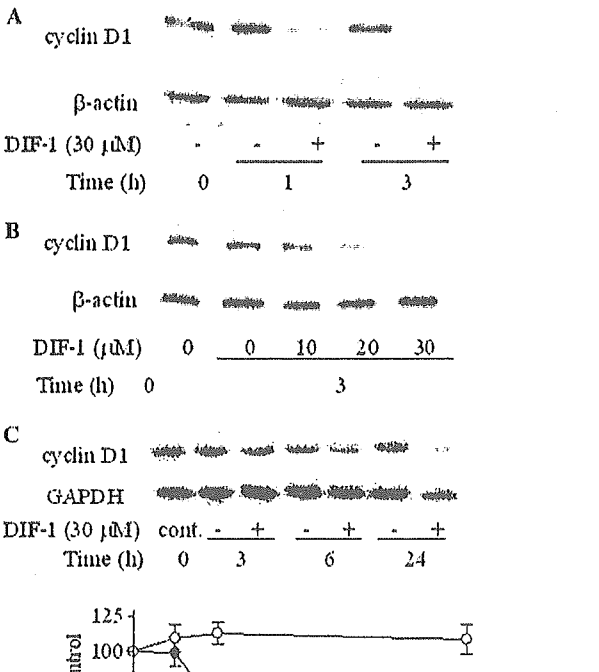

Fig. 1. The effect of DIF-1 on cyclin D1 protein and mRNA. HeLa cells were incubated with or without DIF-1 for the periods indicated. (A,B) Protein samples were collected and subjected to Western blot analysis for cyclin D1. The membrane was reprobed with the anti-β-actin antibody. (A) Time course. (B) Dose dependence. The results are representative of three other experiments. (C) RNA samples were subjected to Northern blot analysis for cyclin D1. The membrane was reprobed with GAPDH probe. The levels of mRNA bands were quantified and are shown as percentages of the control level at time 0. Values are means ± SE of three independent experiments. $^*p < 0.01$ vs. control.

caused by cytotoxicity, because the number of dead cells assessed by the trypan blue exclusion test was not increased by the treatment with DIF-1 (data not shown). Therefore, DIF-1 seemed to have the same effects on cyclin D1 expression as DIF-3 in HeLa cells.

DIF-1 induced the degradation of β-catenin

Since β-catenin is involved in the regulation of cyclin D1 mRNA expression, we examined the effect of DIF-1 on β-catenin expression in HeLa cells. DIF-1 slowly reduced the expression level of β-catenin (Fig. 2A). It took 6 h to significantly reduce the amount of β-catenin, corresponding to the effect on cyclin D1 mRNA shown in Fig. 1C. As demonstrated in Fig. 2B, ubiquitin–proteasome inhibitor ALLN inhibited the loss of β-catenin, indicating that DIF-1 induced ubiquitin-dependent degradation of β-catenin protein. These results suggested that DIF-1 decreased cyclin D1 mRNA by inhibiting the expression of β-catenin.

The effect of DIF-1 on squamous cell carcinoma cells

To clarify whether the effect of DIF-1 is limited to HeLa cells or not, we examined the effect of DIF-1 on squamous cell carcinoma cell line NA. As shown in Figs. 3A and B, DIF-1 reduced mRNA expression level of cyclin D1 and induced the degradation of β-catenin in NA cells. There-

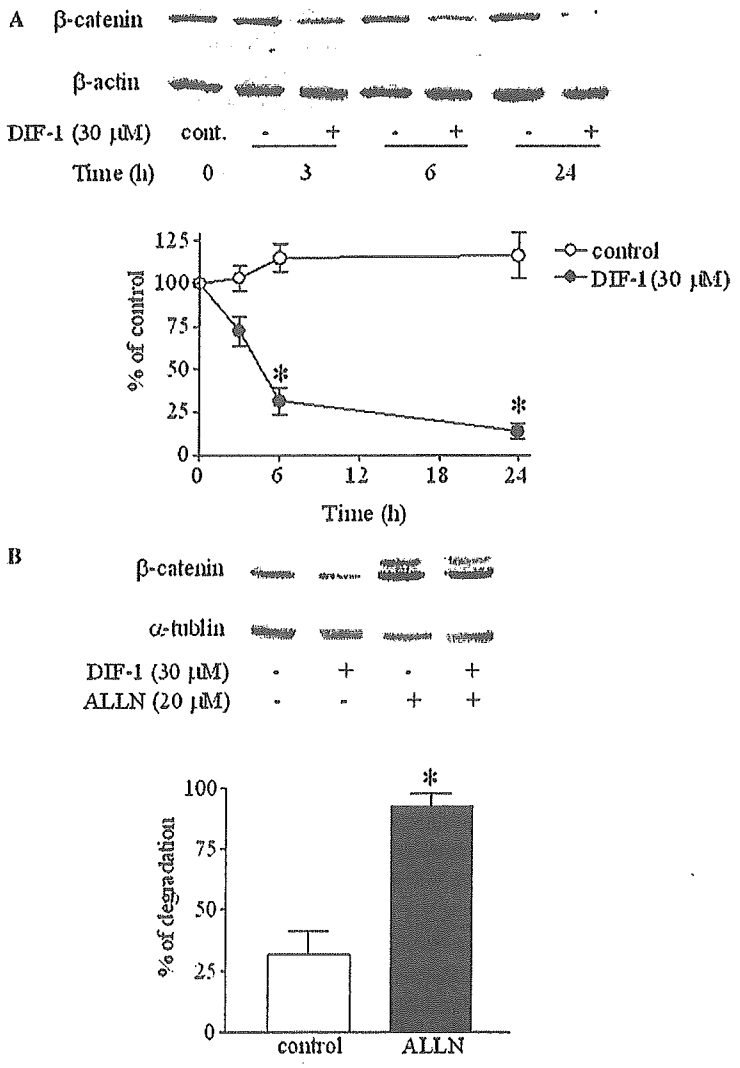

Fig. 2. Degradation of β-catenin induced by DIF-1. (A) Time course. HeLa cells were incubated with or without DIF-1 (30 μM) for the period indicated. Protein samples were separated by 12% SDS–PAGE and immunoblotted with the anti-β-catenin antibody. The membrane was reprobed with the anti-β-actin antibody. The levels of protein bands were quantified and are shown as percentages of the control level at time 0. Values are means ± SE of three independent experiments. *$p < 0.01$ vs. control. (B) Effect of ALLN. HeLa cells were pretreated with ALLN (20 μM) for 1 h and incubated with or without DIF-1 (30 μM) for 6 h. Samples were subjected to Western blot analysis using the anti-β-catenin antibody. The membrane was reprobed with the anti-α-tubulin antibody. The levels of protein bands were quantified and are shown as percentages of the degraded amounts. Values are means ± SE of three independent experiments. *$p < 0.01$ vs. control.

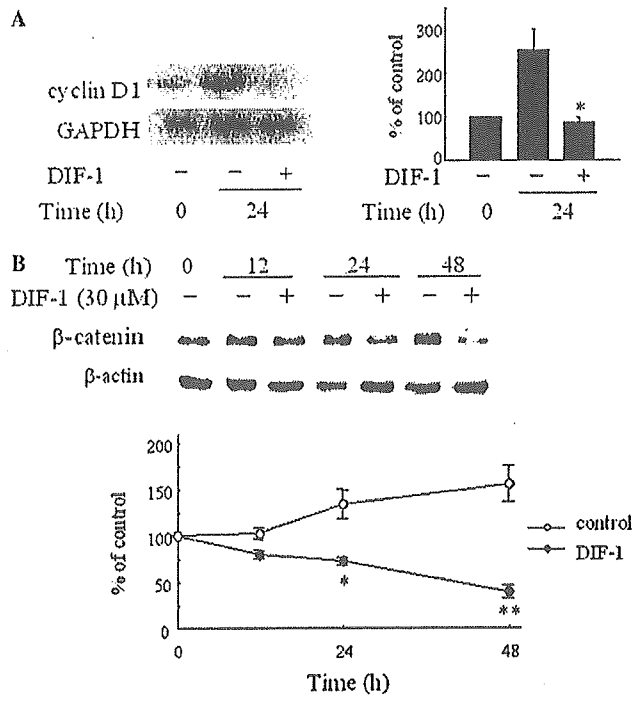

Fig. 3. Effect of DIF-1 on NA cells. (A) Northern blot analysis for cyclin D1. NA cells were incubated with or without DIF-1 (30 μM) for given periods. Total cellular RNAs were extracted and subjected to Northern blot analysis. The membrane was reprobed with GAPDH probe. The expression levels of cyclin D1 mRNA were quantified by densitometry. Values are means ± SE of three independent experiments. $*p < 0.05$ vs.control at 24 h. (B) Western blot analysis for β-catenin. Protein samples were separated by 12% SDS–PAGE and immunoblotted for β-catenin. The membrane was reprobed with the anti-β-actin antibody. The expression levels of β-catenin were quantified by densitometry. Values are means ± SE of three independent experiments. $*p < 0.05$; $**p < 0.01$ vs. control.

fore, these effects are likely to be common among DIF-1-treated tumor cells.

DIF-1 activated GSK-3β

We examined the effect of DIF-1 on GSK-3β in HeLa cells, since GSK-3β has been shown to play a crucial role in the regulation of the stability of β-catenin protein and therefore cyclin D1 gene expression [16,22,23]. Moreover, recently we reported that DIF-1 activates GSK-3β in NA cells [21]. The activity of GSK-3β is regulated by the phosphorylation level of Ser^9 [24,25]. As shown in Fig. 4A, DIF-1 significantly reduced the phosphorylation level of Ser^9 on GSK-3β, indicating that DIF-1 activated this kinase. GSK-3β is a cytosolic protein, however it is translocated into the nucleus when activated. To test whether DIF-1induces nuclear translocation of GSK-3β, we examined the subcellular distribution of GSK-3β after stimulation with DIF-1. The nuclear translocation of GSK-3β was confirmed by immunoblotting. As shown in Fig. 4B, the treatment with DIF-1 markedly increased GSK-3β in the nuclear fraction. To determine the role of GSK-3β in β-catenin degradation induced by DIF-1, the effect of SB-216763, a GSK-3β inhibitor, was examined. Fig. 4C shows that the pretreatment with SB-216763 attenuated the effect of DIF-1 on β-catenin. Taken together, these results suggested that DIF-1 degraded β-catenin through the activation of GSK-3β.

DIF-1 suppressed cyclin D1 promoter activity through the TCF/LEF binding site

Cyclin D1 gene is a target for β-catenin-mediated transcriptional activation, which is mediated by the TCF/LEF binding site in the cyclin D1 promoter [16,23]. To examine the effect of DIF-1 on TCF/LEF transcriptional activity, TOPflash, a TCF/LEF reporter plasmid, was transfected to HeLa cells. As shown in Fig. 5A, DIF-1 significantly reduced the luciferase activity after 6 h stimulation. On the other hand, DIF-1 had no significant effect on luciferase activity when FOPflash, a reporter plasmid containing mutated TCF binding site (a negative control to TOPflash), was transfected to the cells (Fig. 5B). Therefore, DIF-1 seemed to suppress TCF/LEF transcriptional activity.

We subsequently examined the effect of DIF-1 on cyclin D1 promoter activity using cyclin D1 reporter plasmid, the wild-type – 962CD1. As shown in Fig. 6A, DIF-1 significantly reduced the wild-type promoter activity after 6 h stimulation. To examine the role of TCF consensus binding site in DIF action, mutant cyclin D1 promoter, which lacks the TCF consensus site located from −81 to −75 base pairs [16], was employed. DIF-1 exhibited no effect on the mutant promoter activity in HeLa cells (Fig. 6B). These results indicated that DIF-1 inhibited cyclin D1 promoter activity through the TCF/LEF-binding site.

Discussion

In the present study, we showed that DIF-1 promoted β-catenin degradation and also reduced cyclin D1 mRNA expression in a similar time-dependent manner. β-Catenin has been reported to activate cyclin D1 promoter and the sequences related to TCF/LEF consensus binding sites are necessary for the activation [16]. Accordingly, DIF-1 reduced the transcriptional activity of cyclin D1 promoter and the deletion of TCF consensus site abolished this effect. Previously, we reported that DIF-3 induces the degradation of cyclin D1 by stimulation of GSK-3β in HeLa cells [6]. Since β-catenin degradation is triggered by GSK-3β-induced phosphorylation, the activation of GSK-3β by DIF-1 seems to reduce both the protein and mRNA levels of cyclin D1 via the pathways independent of each other. However, as shown in Fig. 4C, DIF-1 slightly but significantly reduced β-catenin levels even in the presence of SB-216763. This result might suggest that not only GSK-3β but also another kinase is involved in β-catenin degradation.

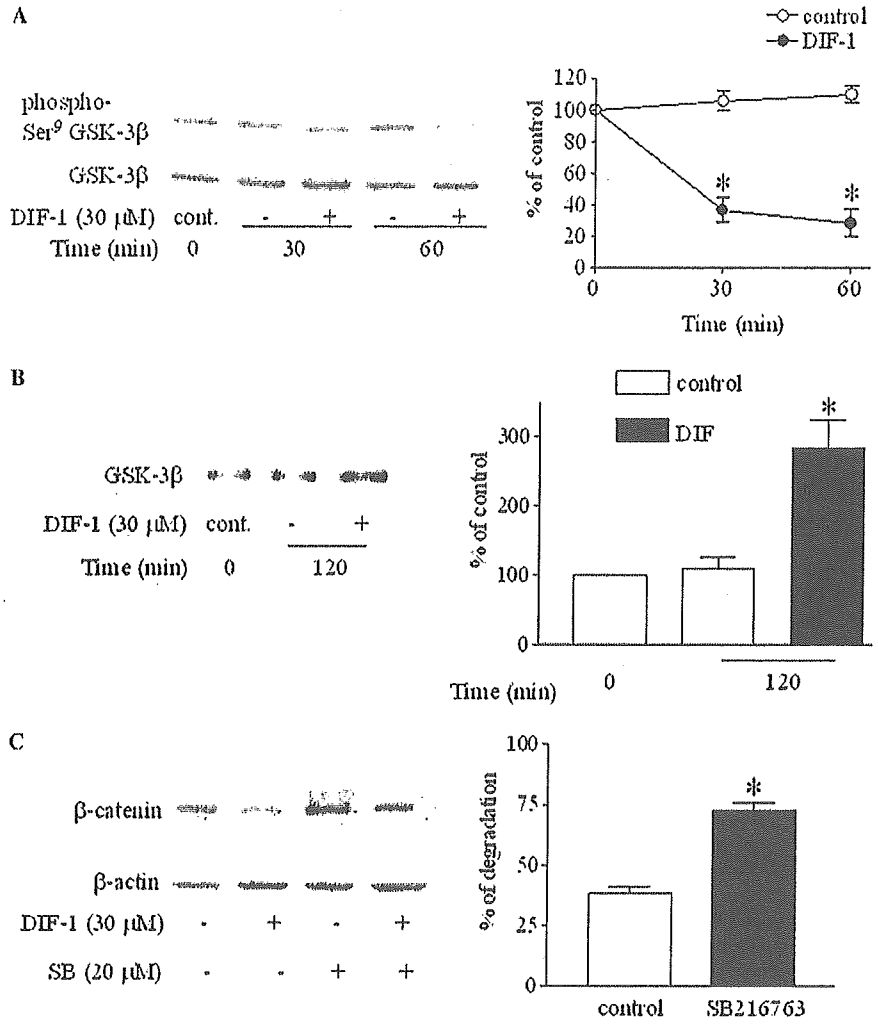

Fig. 4. DIF-1 activates GSK-3β. (A) Phosphorylation of Ser^9 on GSK-3β. HeLa cells were incubated with or without DIF-1 (30 μM) for the periods indicated. Protein samples were separated by 12% SDS–PAGE and immunoblotted with the anti-phospho-GSK-3β (Ser^9) antibody. The membrane was reprobed with the anti-GSK-3β antibody. The levels of protein bands were quantified and are shown as percentages of the control level at time 0. Values are means ± SE of three independent experiments. *$p < 0.01$ vs. control. (B) DIF-1 induces GSK-3β nuclear accumulation. Nuclear proteins were purified from HeLa cells incubated with or without DIF-1 (30 μM) for 2 h. Western blot analysis was carried out using a monoclonal anti-GSK-3β antibody. The levels of nuclear protein bands were quantified and are shown as percentages of the control level at time 0. Values are means ± SE of three independent experiments. *$p < 0.01$ vs. control. (C) Effect of GSK-3β inhibitor on β-catenin degradation. HeLa cells were pretreated with SB-216763 (20 μM) for 1 h and incubated with or without DIF-1 (30 μM) for 6 h. Samples were subjected to Western blot analysis using the anti-β-catenin antibody. The membrane was reprobed with the anti-β-actin antibody. The levels of protein bands were quantified and are shown as percentages of the degraded amounts. Values are means ± SE of three independent experiments.

Cyclin D1 gene (CCND1) is one of the target genes for the Wnt family proteins, a series of secreted lipid-modified signaling proteins [13,16]. GSK-3β and β-catenin are key components of the Wnt signaling pathway. The Wnt proteins induce the expression of a number of genes involved in cell differentiation and proliferation through the inhibition of GSK-3β and the subsequent activation of β-catenin and TCF/LEF [12–15]. DIF-1 activated GSK-3β and degraded β-catenin, which was prevented by SB-216763, suggesting that DIF-1 inhibits an event upstream to GSK-3β in the Wnt pathway. Further, DIF-1 could also influence the expression of other genes regulated by the Wnt/β-catenin pathway.

It has been reported that β-catenin and cyclin D1 are destabilized upon phosphorylation induced by GSK-3β [10,11,22]. However, as shown in Figs. 1 and 2, the degradation of β-catenin was very slow compared with the degradation of cyclin D1. Intracellular distribution of β-catenin and cyclin D1 is different. β-Catenin is localized in the cytosol and cyclin D1 is in the nucleus. As it is known that activated GSK-3β is translocated into the nucleus [24,25], cyclin D1 might be a more susceptible target to activated-GSK-3β than β-catenin.

Recently it has been reported that calmodulin-dependent cyclic nucleotide phosphodiesterase (PDE1) is a pharmacological target molecule for DIF-1 [26]. However, as